ROMA TRE
UNIVERSITÀ DEGLI STUDI

Scuola Dottorale di Biologia

Sezione di Scienze Biolmolecolari e Cellulari

XXV Ciclo

"The role of the *ospB-phoN2* operon in the mechanism of pathogenicity of *S. flexneri*"

"Il ruolo dell'operone *ospB-phoN2* nel meccanismo di patogenicità di *S. flexneri*"

Supervisor I
Prof. M.Casalino

PhD Student
Daniela Scribano

Supervisor II
Prof. M.Nicoletti

PhD School Coordinator
Prof. P.Mariottini

Index

Abstract

In this thesis we have studied the role of the *ospB-phoN2* bicistronic operon in the virulence of *Shigella flexneri*. OspB is, a not fully characterized yet, type III secretion system (T3SS) effector secreted into host cells to subvert cellular and immune functions and promote infection. Here we report evidences that OspB participates at the induction of the severe inflammatory reaction, the hall-mark of bacillary dysentery, at early stages of infection. We found that once secreted into the cytoplasm of host cells, OspB rapidly induces phosphorylation of mitogen-activated protein kinases (MAPKs) Erk1/2 and p38. Early activation of Erk1/2 and p38 leads to the induction of the inflammatory response culminating in massive polymorphonuclear leukocytes (PMNs) infiltration within the colonic mucosa. PMN infiltration, by breaching the epithelial barrier, initially promotes bacterial colonization. On the other hand, 30 min post-infection OspB accumulates within the host cell nucleus where it exerts its functions by modulating expression of pro-inflammatory genes. We propose a working model to try to explain the role of OspB in PMNs transmigration.

Proper protein localization is critical for bacterial virulence. The virulence-associated PhoN2 protein is a periplasmic ATP-diphosphohydrolase (apyrase), involved in *S. flexneri* IcsA-mediated actin-based motility (ABM). IcsA is an autotrasporter protein that is inserted and exposed on the outer membrane (OM) at the old bacterial pole where promote ABM. Here we show that PhoN2 strictly localizes at bacterial poles, where the great majority of bacteria (more that 90%) presenting PhoN2 localized just beneath IcsA. PhoN2 was found to be polarly localized also in a *phoN2*-complemented *Escherichia coli* K-12 strain, indicating a conserved mechanism of PhoN2 delivery across species. Analysis of deletion and point mutations encompassing the N-terminal polyproline (^{41}ILPPPPAE^{48}) and C-terminal regions of PhoN2 indicated that the PPPP motif and the Y155 residue play a pivotal role in the polar localization of PhoN2, in its proper folding and stability, in the correct exposition of IcsA and in apyrase activity. Two-hybrid and cross-linking experiments proved OmpA as a strong interactor of PhoN2. Interestingly, neither IcsA nor OmpA are required for PhoN2 polar localization, while the lack of OmpA induces IcsA exposition over the entire bacterial length. A model is presented to explain how the PhoN2-OmpA interaction allows proper IcsA exposition and ABM.

Next, the finding of a PhoN2-OmpA interaction prompted us to investigate the role of OmpA on the virulence of *S. flexneri*. An *ompA* mutant of wild-

type *S. flexneri* 5a strain M90T (strain HND92) was shown to be severely impaired in cell-to-cell spread since it failed to plaque on HeLa cell monolayers. Nevertheless, the *ompA* mutant displayed IcsA exposed across the entire bacterial surface although it was able to produce proper F-actin comet tails, indicating that the aberrant IcsA exposition at bacterial lateral surface did not affect proper activation of actin-nucleating proteins, and suggesting that the absence of OmpA likely unmasks IcsA at bacterial lateral surface. Moreover, the *ompA* mutant was able to invade and to multiply within HeLa cell monolayers, although internalized bacteria were found to be entrapped within the host cell cytoplasm. We found that the *ompA* mutant produced significantly less protrusions than the wild-type strain, indicating that this defect could be responsible of its inability to plaque. Complementation of the *ompA* mutation clearly indicated that a functional OmpA protein is required and sufficient for proper IcsA exposition, plaque and protrusion formation.

Riassunto

In questa tesi abbiamo studiato il ruolo dell'operone bicistronico *ospB-phoN2* nel meccanismo di virulenza di *Shigella flexneri*. OspB è un effettore secreto dal sistema di secrezione di tipo terzo (T3SS) il cui ruolo non è stato ancora del tutto caratterizzato. OspB, quando viene rilasciato all'interno della cellula ospite, è in grado di modulare la fisiologia cellulare e la risposta immunitaria promuovendo l'instaurarsi dell'infezione. Il nostro studio evidenza che OspB ha un ruolo nell'induzione della imponente reazione infiammatoria, caratteristica saliente della dissenteria bacillare, agendo negli stadi precoci dell'infezione. Quando viene secreto nel citoplasma della cellula ospite OspB induce rapidamente la fosforilazione e quindi l'attivazione di Erk1/2 (*Extracellular response kinases*) e p38 che rappresentano due principali MAP (*mitogen-activated protein*) chinasi coinvolte nella attivazione della risposta cellulare ad uno stimolo infiammatorio. Infatti, quando Erk1/2 e p38 sono attivate, attraverso una cascata di trasduzione del segnale, inducono l'attivazione della risposta infiammatoria che culmina con il potente richiamo di leucociti polimorfonucleati (PMN) nel sito d'infezione. L'infiltrazione dei PMN nel tessuto causa la distruzione dell'integrità dell'epitelio intestinale, aprendo vie d'accesso alla sottomucosa, sfruttate dai batteri per la colonizzazione del tessuto, nelle fasi precoci dell'infezione. Successivamente OspB si localizza nel nucleo della cellula ospite e in questo sito esplica la sua funzione modulando l'espressione dei geni pro-infiammatori. I nostri risultati ci hanno permesso di proporre un modello che spiega il meccanismo attraverso il quale OspB attiva la risposta infiammatoria dell'ospite.

L'azione di alcuni fattori di virulenza dipende dalla loro specifica localizzazione all'interno della cellula batterica. PhoN2 è una proteina periplasmica associata alla virulenza di *S. flexneri*, è una ATP difosfoidrolasi che è coinvolta nel meccanismo di movimento di *S. flexneri*. Tale meccanismo si basa sulla polimerizzazione d'actina della cellula ospite (ABM), e richiede l'espressione del fattore di virulenza IcsA che si inserisce e si espone sulla membrana esterna, al polo vecchio del batterio. Il nostro studio dimostra che PhoN2 si localizza, nel periplasma, ai poli batterici, inoltre la maggior parte dei batteri presenta PhoN2 localizzata sotto la proteina IcsA. La localizzazione polare di PhoN2 è mantenuta anche in un ceppo di *Escherichia coli*, a cui è stato inserito *in trans*, il gene *phoN2*, indicando che esiste un meccanismo di esporto al polo batterico conservato in entrambe le specie. PhoN2 presenta una sequenza ricca in

proline nella regione N-terminale (^{41}ILPPPPAE^{48}) e i domini del sito catalitico nella regione C-terminale. Attraverso delezioni e sostituzioni amminoacidiche sul motivo PPPP e nel sito catalitico abbiamo dimostrato che il motivo PPPP e la tirosina 155 (Y155) sono residui necessari alla struttura tridimensionale di PhoN2. Di conseguenza tali residui sono necessari nella stabilità della proteina, nell'attività enzimatica e indirettamente nel processo di localizzazione di IcsA al polo batterico. Tramite il saggio del doppio ibrido in lievito abbiamo dimostrato che PhoN2 interagisce con la proteina della membrana esterna OmpA. Sia OmpA che IcsA non sono coinvolte nel meccanismo di localizzazione polare di PhoN2, viceversa la mancanza della proteina OmpA causa una aberrante esposizione di IcsA su tutta la superficie batterica. Noi proponiamo un modello attraverso il quale l'interazione tra PhoN2 e OmpA consente la corretta esposizione di IcsA al polo, permettendo, quindi, un corretto movimento del batterio all'interno della cellula ospite.

La dimostrazione che OmpA interagisce con il fattore di virulenza PhoN2 ci ha indotto a studiare il ruolo di tale proteina nel meccanismo di patogenicità di *S. flexneri*. Il mutante nullo nel locus *ompA* (ceppo HND92) mostrava un movimento intercellulare aberrante poiché non produceva placche di lisi su monostrati di cellule HeLa in coltura. Anche se il mutante nullo per *ompA* presentava IcsA esposta su tutta la superficie batterica era in grado di indurre polimerizzazione d'actina, quindi l'esposizione aberrante di IcsA non influenzava la capacità di tale proteina di reclutare le proteine eucariotiche responsabili della polimerizzazione d'actina. Questo ci ha suggerito che OmpA potrebbe svolgere un ruolo nel mascherare IcsA sulla superficie batterica senza agire sulla capacità di tale proteina di indurre polimerizzazione d'actina. Tramite saggi di invasione di cellule HeLa in coltura, abbiamo osservato che il ceppo HND92 aveva un tasso di invasione inferiore rispetto al ceppo parentale M90T e che non era in grado di formare le protrusioni. Le protrusioni permettono la diffusione del batterio da una cellula alla cellula adiacente. Questo risultato potrebbe spiegare l'inabilità del mutante *ompA* di produrre le placche di lisi su monostrati HeLa. L'inserimento *in trans* del gene *ompA* nel ceppo HND92 ha dimostrato che la proteina OmpA è richiesta per la corretta esposizione di IcsA nella membrana esterna, per la formazione delle protrusioni e quindi per la produzione di placche.

Introduction

Shigella flexneri is a Gram-negative facultative intracellular pathogen that leads to severe inflammatory colitis called bacillary dysentery (or shigellosis), a major public-health problem in developing countries. After its passage through the stomach and small intestine, *S. flexneri* reaches the colonic mucosa where infects the colonic epithelium via M cell translocation. Once *S. flexneri* is endocytosed by M cells, bacteria are transocytosed toward the M cell pocket and invade resident macrophages and dendritic cells, where they disrupt vacuolar membranes and then disseminate into and replicate within the cytoplasm. Bacterial multiplication within macrophages results in a massive inflammatory response (the hallmark of shigellosis) and cell death (apoptosis). Macrophage apoptosis induces synthesis and release of proinflammatory cytokines which in turn leads to recruitment polimophonuclear leukocytes (PMNs) at the site of infection (Fig. 1). Once free in the sub-mucosa, *S. flexneri* induces its internalization at baso-lateral sites of the polarized epithelial epithelium (Sasakawa, 2010). After internalization into epithelial cells, *S. flexneri* rapidly disrupts surrounding vacuolar membrane, multiplies through the cytoplasm and diffuses to adiacent cells by inducing F-actin polymerization at one pole (the old pole) of the bacterium. Thus, macrophage cell death, invasion of and multiplication within epithelial cells, cell-to-cell spreading, demise of the host epithelium and alteration of the host inflammatory response are major pathogenic events that lead to shigellosis (Makino *et al.*, 1986, Sansonetti *et al.*, 1986, Clerc *et al.*, 1987, Bernardini *et al.*, 1989, Sansonetti *et al.*, 2001).

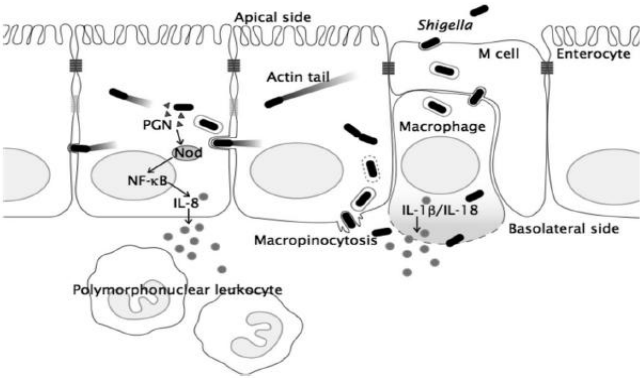

Fig. 1. A model for *S. flexneri* infection of intestinal epithelial cells.

The ability of *S. flexneri* to move within the cytoplasm of invaded epithelial cells and to diffuse the infection to adjacent cells of the intestinal mucosa requires the expression and polar surface exposition of IcsA (VirG), a 110-kDa autotransporter protein encoded on the *S. flexneri* large virulence plasmid (Bernardini *et al.*, 1989). Once translocated across the outer membrane (OM), IcsA exposes its N-terminal α-domain (the passenger domain) on the bacterial surface, forming a cap exclusively at the old bacterial pole (Goldberg *et al.*, 1993, Goldberg *et al.*, 1994). Exposed IcsA, by interacting with neural Wiskott-Aldrich syndrome protein (N-WASP) and vinculin, induces F-actin polymerization by activating host Arp2/3 complex, which induces polymerization of host globular actin into filamentous actin (Suzuki *et al.*, 1998 , Cossart, 2000, Charles *et al.*, 2001, Goldberg, 2001, May and Morona 2008, Heindl *et al.*, 2010) (Fig. 2). Although the mechanism driving the polar localization of IcsA has not been fully elucidated, experimental evidence indicates that IcsA likely inserts directly at the old bacterial pole (Goldberg *et al.*, 1993, Fukuda *et al.*, 1995, Steinhauer *et al.*, 1999).

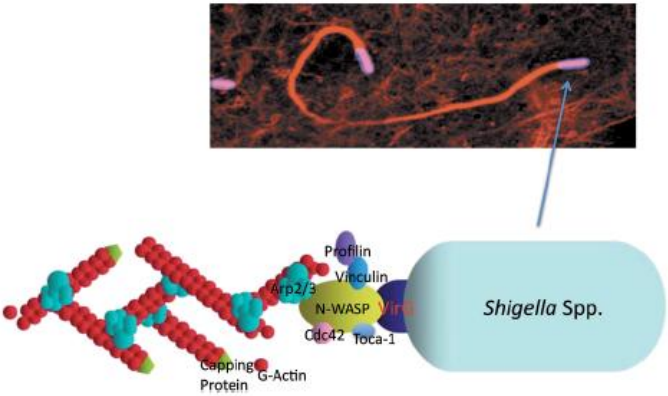

Fig. 2. The actin-dependent Shigella motility. A confocal immuno-fluorescence image of actin tails. Bottom, the machinery required for bacterial motility, VirG/IcsA, N-WASP, Arp2/3 complex, profilin, and Toca-1, accumulates at the old bacterial pole (Sasakawa 2010).

Furthermore, IcsA-mediated actin-polimerization is essential for *S. flexneri* to diffuse to adjacent cells via protrusion formation. Protrusions are membrane-bound cell extensions that are driven by the bacterium to propel itself into adjacent cells. Protrusions, which may extend tens of microns from the cellular surface, are characterized by the presence of a bacterium at its tip (Bernardini *et al.*, 1989). By a process which likely resembles macropinocytosis, contact with the membrane of an adjacent cell is followed by uptake of the bacterium (Kadurugamuwa *et al.*, 1991), leading to the spreading of the infection to neighbouring epithelial cells. Several host cell proteins have been implicated in protrusion-mediated *Shigella* cell-to-cell spreading, suggesting that a distinct set of actin regulatory factors likely interacts with motile bacteria after they contact the plasma membrane (Haglund and Welch 2011). Although actin polymerization and assembly are required for protrusion formation, the specific mechanism responsible for this phenomenon is poorly defined. It has been recently reported that actin nucleation in protrusion formation might be independent of the activity of the Arp2/3 complex and that protrusion formation and inter-cellular spreading depend on actin polymerization that requires the activation of the Diaphanous formin Dia (Heindl *et al.*, 2010). Formins are a family of ubiquitous expressed proteins that, in contrast to the Arp2/3 complex, initiate *de novo* actin polymerization leading to cross-linking of actin polymers in parallel arrays (Heindl *et al.*, 2010).

Apyrase (PhoN2) is an ATP-diphosphohydrolase encoded by *phoN2* (*apy*), a gene located on a highly conserved region (the *ospB-phoN2* operon) of *Shigella* species and related enteroinvasive *Escherichia coli* (EIEC) strains (Santapaola *et al*., 2002). *ospB* and *phoN2* are co-transcribed as a 2 kb bicistronic, temperature-regulated mRNA from an upstream promoter that precedes *ospB* (Santapaola *et al.*, 2002). OspB is a type III secretion system (T3SS) secreted effector and transcription of the *ospB-phoN2* operon is regulated by the VirF/VirB cascade and by MxiE, in concert with IpgC (Buchrieser *et al.*, 2000, Le Gall *et al.*, 2005, Santapaola *et al.*, 2006). Even if PhoN2 is not a secreted effector, *phoN2* transcription is also up-regulated by MxiE when the T3SS system is activated, suggesting that PhoN2 may be relevant in post-invasion events and that both PhoN2 and OspB might be functionally related (Santapaola *et al*., 2006).

The purpose of this study was to evaluate the contribution of OspB and PhoN2 to the virulence of *S. flexneri*. It has been recently reported that OspB, once secreted into host cell, translocates into the nucleus where interacts with retinoblastoma protein thus participating at the remodeling of chromatin which leads to reduced inflammatory cytokines production and

to modulate the innate immune response (Zurawski *et al.*, 2009). Moreover, it has been also shown that OspB, by activating the mitogen-activated extracellular kinase (MEK)/Erk1/2 pathway, leads to up-regulation of neutrophil attractant–hepoxilin A3 (HXA3) which induces trans-epithelial migration of polymorphonuclear leukocytes (PMNs) and increases the inflammatory response (Kohler *et al.*, 2002, Mumy *et al.*, 2008, Zurawski *et al.*, 2009). Thus, it is conceivable that OspB may play a dual role depending on the stage of infection. At an early stage, OspB appears to induce inflammation while at late stages (after its nuclear translocation) it appears to attenuate the inflammatory response.

In this study, we evaluated the role of OspB in the inflammatory response at early stages of infection. First, we confirmed that OspB is involved in the inflammatory response since an *ospB* null-mutant of the wild-type *S. flexneri* 5a strain M90T failed to induce the levels of the inflammatory response seen with wild-type, in the Serény test model of infection. Moreover, we found that OspB activates both Erk1/2 and p38 signaling pathways at early stages of infection. Since it is known that phosphorylation of Erk1/2 and p38 leads to the activation of complex pro-inflammatory pathways leading to PMNs migration, we hypothesized that OspB might play also a role in PMNs migration to the site of infection. Experiments are underway to unravel this point. A model is presented to explain this hypothesis.

PhoN2 is an ATP-diphosphohydrolase (apyrase) so far isolated only in *Shigella* ed EIEC. Basing on its deduced biochemical structure, PhoN2 was considered a periplasmic protein. Here we produced experimental evidence proving apyrase as a periplasmic protein of *S. flexneri*. Moreover, we have previously shown that PhoN2 is required, in a deoxynucleotide triphosphate-hydrolyzing activity-independent manner, for efficient inter-cellular spreading since a non polar *phoN2* mutant of the wild-type *S. flexneri* strain M90T presented altered polar IcsA exposition, aberrant actin-based motility and a small plaque phenotype (Santapaola *et al.*, 2006). The mechanism by which PhoN2 influences the polar exposition of IcsA has not been fully elucidated yet. However, since PhoN2 possesses an exposed N-terminal polyproline (^{43}PPPP^{46}) motif and proline-rich motifs have been reported to be involved in inter- and intra-molecular interactions, in protein folding and essential for virulence of various intracellular pathogens (Neibuhr *et al.*, 1997, Suzuki and Sasakawa, 2001, Babu *et al.*, 2002, Ansai *et al.*, 2002, Makde *et al.*, 2007), we hypothesized that PhoN2 might directly interact with IcsA or indirectly with other unknown

accessory outer membrane (OM) proteins necessary in assisting the correct polar exposition of IcsA (Santapaola *et al.*, 2006).
The data presented in this work are based on the serendipitous discovery that the PhoN2 periplasmic pool localizes at either one (the old pole) or at both poles of *S. flexneri*. Here we analyzed the role of definite PhoN2 regions on PhoN2 polar localization, on expression of apyrase activity and protein stability. Polar localization of PhoN2 occurred also when PhoN2 was expressed in a *E. coli* K-12 genetic background, indicating a conserved mechanism of PhoN2 polar localization in both species. Analysis of deletion and point mutations encompassing the phoN2 DNA region encoding the N-terminal polyproline PPPP stretch, allowed us to demonstrate the pivotal role of this motif on the polar localization of PhoN2, on its stability and on the expression of its catalytic activity.
PhoN2 is a member of the class A of nonspecific acid phosphohydrolases (A-NSAPs) (Rossolini *et al.*, 1998). A-NSAPs share as common features an N-terminal PPPP motif and conserved amino acid residues over their C-terminal domain (Rossolini *et al.*, 1998, Ansai *et al.*, 2002, Babu *et al.*, 2002, Sarli *et al.*, 2005) (Fig. 3).

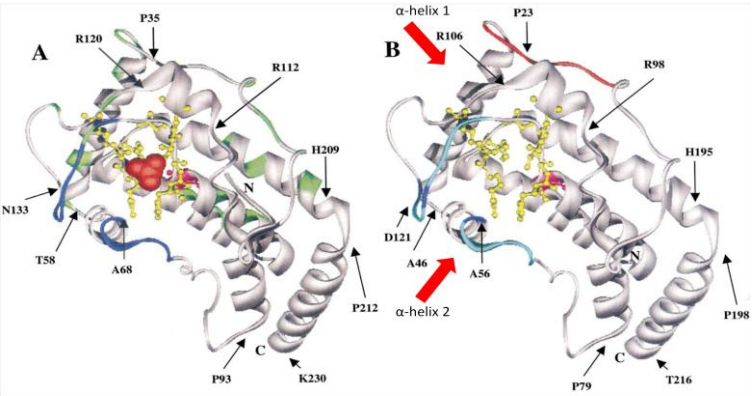

Fig. 3. The 3D structure of *S. flexneri* PhoN2 (B)obtained by threading using Swiss-Model with *E. blattae* EBPase (A) as PDB template (1D2T). The EBPasi is shown as a monomer complexed with sulfate. Residues from the acitve site, conserved in both structures, are represented as ball and stick structure in yellow. The dimer and trimer contact residues are highlighted in green in A. The quite different sequences implicated in substrate binding are shown in blue in A and in cyan in B. the poly-proline region is colored in red in B. Red arrows indicate α-helices 1 and 2. Adapted from Babu *et al.*, 2002.

Finally, we showed that the PhoN2 PPPP motif, along with the Y155 residue, is involved in the structural conformation of PhoN2, leading to the proper folding of the protein, in its stability, and consequently in its polar localization and in the expression of its catalytic activity.
To determine possible interactors of PhoN2 needed for the correct delivery of IcsA at the old bacterial pole and for PhoN2 polar localization, two-hybrid technology and cross-linking experiments were conducted and OmpA was found as a strong interaction partner of PhoN2. OmpA is a 35 kDa monomeric protein embedded in the bacterial OM as a β-barrel protein, highly conserved among Gram-negative bacteria (Krishnan and Prasadarao 2012). OmpA is thought to play a pivotal role, along with other bacterial components, in the structural integrity of the OM and it has been reported to be an important virulence factor of several human pathogens (Smith *et al.*, 2007, Reusch 2012, Krishnan and Prasadarao 2012). Furthermore, in an experimental animal model, OmpA of *S. flexneri* 2a has been identified as a novel molecule coordinating the innate and adaptive immune responses, strongly indicating that OmpA may also represent a promising antigen in vaccine development (Pore *et al.*, 2009, Pore *et al.*, 2012). Since, in spite of its importance, to date no reports have documented the role of OmpA on the virulence of *S. flexneri*, we decided to carry out experiments addressed to elucidate this point. Here we demonstrated that OmpA plays a pivotal role in the virulence of *S. flexneri*, since we found that OmpA is absolutely required for proper IcsA localization and exposition on the OM, plaque and protrusion formation. These results were published in PLoS One 2012 7:49626.
Basing on these results, we propose a model to explain how PhoN2, by interacting with OmpA, participates to the formation of the classical IcsA caps in *S. flexneri*.

Results

OspB is involved in the modulation of host inflammatory response

In a previous study we have shown that the *S. flexneri ospB* gene is a virulence-associated gene encoding a T3SS-secreted effector and that its expression is under the control of the VirF/VirB and MxiE regulatory network (Santapaola *et al.*, 2006). Although the precise mechanism of OspB has not been fully elucidated yet, it has been recently reported that OspB might play a role in the host inflammatory response, the hallmark of bacillary dysentery (Zurawski *et al.*, 2009). To confirm whether OspB is involved in *S. flexneri* induction of the inflammatory response, we performed Serény tests on Guinea pigs (Serény, 1957). Animals (three for each group) were infected with the wild-type *S. flexneri* 5a strain M90T, with its isogenic *ospB* deletion derivative strain HND201, with HND201 complemented with plasmid pOspB and with the non-invasive *virB*-null mutant HND53 (Table 1) included in the experiment as a negative control (Santapaola *et al.*, 2006). Exponentially-growing bacterial suspensions were used to infect each animal. Briefly, 30 µl of each bacterial suspension, containing about 5.0×10^8 bacteria, were used to infect one eye of each animal and symptoms were monitored daily for four days. The degree of keratoconjunctivitis was ranked on the basis of time of development, severity, and rate of clearance of symptoms. The results obtained (Table 2) clearly indicated a dramatic reduction in the intensity of keratoconjunctivitis and a delayed onset of symptoms for guinea pigs infected with the *ospB* mutant strain HND201, compared to parental strain. The observed delay in the emergence of symptoms of keratoconjunctivitis and inflammation was indeed due to the lack of OspB since complementation of HND201 with plasmid pOspB almost completely restored the inflammatory response seen with parental strain. As expected, no inflammation was observed when eyes were infected with the non-invasive *virB* mutant (strain HND53).

These results clearly indicated that, in this model of infection, OspB is involved in modulating the severity of the *S. flexneri* inflammatory response.

Table 1. Bacterial/yeast strains and plasmids used in this study.

Strain or plasmid	Relevant genotype or characteristic(s)	Source or ref.
strains		
M90T	wild-type *S. flexneri* serotype 5a	Sansonetti *et al.*1982
HND115	M90T *ΔphoN2*;susceptible	Santapaola *et al.*2006
HND201	M90T *ΔospB*;susceptible	Santapaola *et al.*2006
HND53	M90T *ΔvirB*;susceptible	Santapaola *et al.*2006
HNDHA10	M90T *phoN2*::HA;susceptible	This thesis
HND549	M90T *ospB*::3×FLAG;susceptible	Santapaola *et al.*2006
HND92	M90T *ΔompA*; Km^r	This thesis
HND93	HND115 *ΔompA*; Km^r	This thesis
SC560	M90T *ΔicsA*::Ω; Sm^r	d'Hauteville and Sansonetti 1992
BS176	M90T 220-kb pINV cured; Sm^r	Sansonetti *et al.*1981
DH10b	E.coli K-12	Gibco BRL
XL1-blue	E.coli K-12	Stratagene
ME9062	E.coli K-12 BW25113	Keio collection
JW0940	E.coli K-12 ME9062 *ΔompA*; Km^r	
AH109	S.cerevisiae	Clonthec
Plasmids		
pGEM-T	Cloning vector, Ap^r	Promega
pSU315	Plasmid carrying HA epitope and Km cassette; Km^r	Uzzau *et al*. 2001
pKD46	λRed helper plasmid; Ap^r	Datsenko and Wanner 2000
pCP20	FLP helper plasmid; Ap^r Cm^r	
pBAD28	Arabinose-inducibile expression vector; Ap^r Cm^r	Guzman *et al.* 1995
pACYC184	Low copy number cloning vector; Tc^r Cm^r	Fermentas
pOspB	pACYC184 *ospB*; Tc^r	This thesis
pOspBF	pACYC184 *ospB*::3xFLAG; Tc^r	This thesis
pOA	pACYC184*ompA*; Cm^r	This thesis

pOmpA	pACYC184 *ompA*; Tc^r	This thesis
pAAAOmpA	pOmpA derivative encoding ^{183}AAAAA^{187} substitution	This thesis
pHND10	pBAD28 *phoN2*::HA; Ap^r Cm^r	This thesis
$pHND11_{\Delta 79\text{-}223}$	pHND10 derivative carrying 144 nt in-frame deletion 79-223	This thesis
$pHND23_{SPPP}$	pHND10 encoding P43S substitution	This thesis
$pHND14_{PSPP}$	pHND10 encoding P44S substitution	This thesis
$pHND15_{PPSP}$	pHND10 encoding P45S substitution	This thesis
$pHND16_{PPPS}$	pHND10 encoding P46S substitution	This thesis
$pHND19_{R192P}$	pHND10 encoding R192P substitution	This thesis
$pHND21_{Y155A}$	pHND10 encoding Y155A substitution	This thesis
pGBKT7	Cloning vector; TRP1; Km^r	Clontech
pGBKT7/phoN2	pGBKT7 carrying GAL4 DNA-BD fused with *phoN2*; TRP1; Km^r	This thesis
pGADT7-Rec	SmaI linearized coning vector used to clone DNA library of M90T; LEU2, Apr	Clontech

Table 2. Role of *ospB* in inflammation

Strain	24 h	48 h	72 h	96 h
WT	2	3/4	4	3
ospB	1	2	2	~3
ospB/pOspB	1/2	3	3	2/3
virF	0	0	0	0

30 µl of exponentially-growing bacterial suspensions (approximately 5.0×10^8 bacteria) were used to infect one eye of guinea pigs. Symptoms were monitored daily for four days. The degree of keratoconjunctivitis was ranked on the basis of time of development, severity, and rate of clearance of symptoms, if any, with the following scores: 0, no reaction or mild irritation; 1, mild keratoconjunctivitis or late development and/or rapid clearing; 2, keratoconjunctivitis, but not purulent; 3, fully developed keratoconjunctivitis with purulence; 4, eyes as in 3, but unusually swollen with excessive purulence.

Expression of *S. flexneri ospB* gene in infected HeLa cell monolayers and OspB localization in the host cell

To find best experimental conditions to use for localize OspB within host cell compartments, we measured, by quantitative Real-Time PCR analysis, *ospB* transcription in HeLa cells infected with parental M90T strain. Briefly, semi-confluent monolayers were infected with strain M90T and, at selected time points after infection, total mRNA was extracted and the relative expression of *ospB* was measured, 30 min to 180 min post-infection, as previously described (Nicoletti *et al.*, 2008). As shown in Figure 4, the intracellular expression of *ospB* reaches a peak at 60 min post-infection, and decreased gradually over the time. Next, we evaluated the intracellular localization of OspB on HeLa cells. To this end, semi-

confluent HeLa cell monolayers were infected with the *ospB* mutant strain HND201 complemented with plasmid pOspBF (a pACYC184-based recombinant plasmid carrying the *ospB* gene fused at its C-terminus to the 3×FLAG tag; Table 1), and samples were analyzed by indirect immune-fluorescence. Interestingly, accumulation of OspB within the host nucleus was observed already 30 min post-infection (Fig. 5) indicating that, once secreted into the cytosol, OspB rapidly moves to the nucleus. Remarkably, in silico analysis failed to evidence canonical nuclear localization signals (NLS) in OspB, indicating that OspB might directly interact with host proteins presenting canonical NLS to translocate within the nucleus.

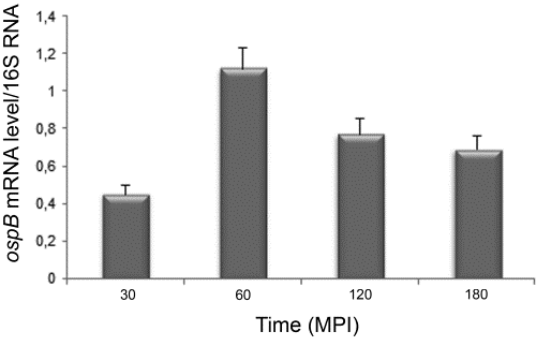

Fig. 4. Expression of *S. flexneri ospB* gene during cell invasion. Semi-confluent HeLa cell monolayers were infected with the wild-type *S. flexneri* M90T strain (MOI=150). At the indicated time points post-infection, total mRNA was extracted, cDNAs were synthesized and expression was measured by quantitative Real-Time PCR. Bars depict relative levels of *ospB* mRNAs, normalized to the levels of the constitutively expressed house-keeping gene *rrsA* (16S rRNA). Values represent mean±SD of three independent experiments, in duplicate.

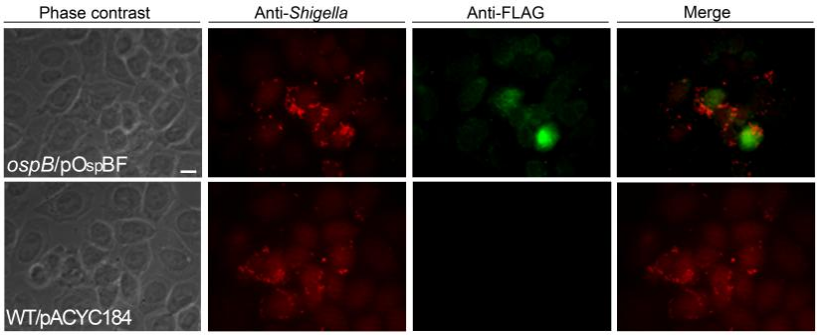

Fig. 5. OspB localizes within host nucleus at early times of infection. Semi-confluent HeLa cell monolayers were infected with the *ospB* mutant HND201 complemented with plasmid pOspBF (ospB/pOspBF) (Table 1), at a MOI of 150. At suitable intervals post-infection, cell monolayers were fixed and labeled with antibodies against the LPS of the *S. flexneri* serotype 5a strain M90T (red), and anti-FLAG (green). Images shown above were taken 30 min post-infection, recorded with a Leica camera and processed using Qwin software (Leica DMRE). Scale bar = 10 µm.

OspB activates the MAPK signalling pathways in Caco-2 cultured intestinal epithelial cells

Several pathogenic bacteria are able to modulate host MAPK signalling pathways to colonize and multiply within the susceptible host (Shan *et al.*, 2007, Bhavsar *et al.*, 2007). Accordingly with the timing of the release of OspB in infected host cells cytoplasm (data not shown), the role of OspB in the induction of MAPK signalling pathways was determined at early stages of infection. Semiconfluent monolayers of the colonic epithelial Caco-2 cell line were infected (MOI=150) with the wild-type, the *ospB* mutant strain HND201, and HND201 complemented with pOspB. At 5, 15, 30 and 60 min post-infection whole cell extracts were prepared and analyzed by Western blot by using polyclonal anti-phospho-Erk1/2 and anti-phospho-p38 antibodies. Anti-total-Erk1/2 and anti-total-p38 antibodies were used in order to detect the total level of Erk1/2 and p38 present in each sample as well as to ascertain that equal amounts of proteins were loaded in each well (Fig. 6A and B). The intensity of each band was quantified by densitometric analysis and expressed as the ratio between phosphorylated

and total protein. Interestingly, 5 min post-infection we found a remarkable reduction in the amounts of phosphorylated Erk1/2 in all samples analyzed. On the other hand, at 15 min time point onward, compared to cells infected with the wild-type strain, cells infected with the *ospB* mutant HND201 showed approximately 50% less phosphorylated Erk1/2 (Fig. 6C). Remarkably, a more dramatic reduction of the amount of phospho-p38 (about. 70%) was detected at 5 and 15 min post-infection in cells infected with the *ospB* mutant (Fig. 6D). Differently from pErk1/2, phospho-p38 levels returned to the values observed in cells infected with wild-type at 60 min post infection (Fig. 6). As expected, the ability to modulate phosphorylation of Erk1/2 and p38 at almost wild-type levels was restored when HND201 was complemented with plasmid pOspB (Fig. 6). These results indicated that OspB, during its translocation to the nucleus, someway targets cytosolic MAPKs, Erk1/2 and p38 inducing their activation at early stages of infection. Since it is known that phosphorylation of ERK1/2 and p38 leads to the activation of complex pro-inflammatory pathways leading to PMNs migration, we hypothesized that OspB might play also a role in PMNs migration to the site of infection.

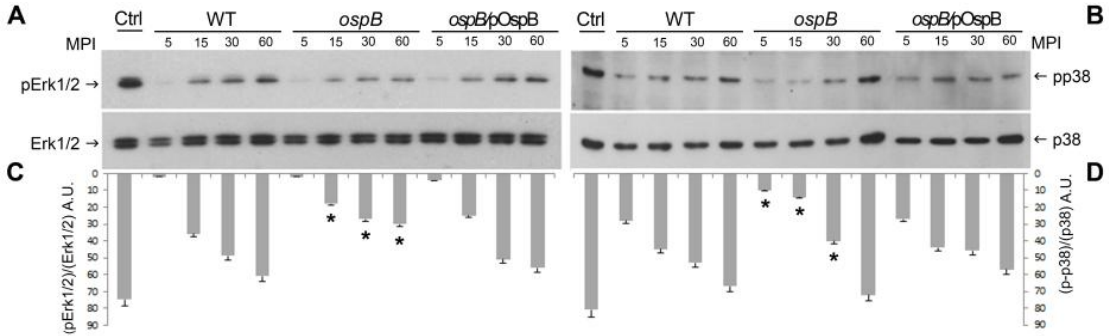

Fig. 6. OspB induces Erk1/2 and p38 phosphorylation. Figure shows representative images of Western blot analysis. Caco-2 cells were infected with wild-type (WT), the *ospB* mutant strain HND201 (*ospB*), and its complemented-derivative strain (*ospB*/pOspB). At the indicated time points post-infection, cells were lysed and whole protein extracts separated on a 10% SDS-PAGE. After transfer to PVDF membranes, membranes were probed with anti-phospho-Erk1/2 and anti-phospho-p38 antibodies (panel A and B, respectively). Membranes were also probed with the corresponding anti-total-Erk1/2 and anti-total-p38 antibodies to assure the loading of equal amounts of proteins (Panels C and D, respectively). Bars represent the means of densitometric analysis (ImageJ software) of three independent experiments. Data are expressed as arbitrary units. Asterisks (*) indicate a statistically significant difference compared with to wild-type (Student's t-test; *P* values < 0.05). Uninfected Caco-2 cells were used as control (Ctrl).

Periplasmic PhoN2 (apyrase) polarly localizes in *S. flexneri* and *E. coli* cells

We have previously shown that PhoN2 (apyrase) is a virulence-associated factor required for efficient *S. flexneri* cell-to-cell spreading (Santapaola *et al.*, 2006). In spite of experimental and structural evidences indicating PhoN2 as a periplasmic protein (Bhargava *et al.*, 1995, Babu *et al*., 2002), a conclusive demonstration has never been reported. To definitively settle this point, we analyzed protein extracts of different bacterial compartments (periplasm, cytosol and membrane fractions) of the wild-type strain M90T, grown at 30°C and at 37°C, in the presence of the Congo red dye in order to activate *phoN2* MxiE-regulated transcription (Le Gall *et al.*, 2005, Santapaola *et al.*, 2006). Proteins were separated by SDS-PAGE and analyzed by Western blot using mouse polyclonal antibodies raised against PhoN2 (Santapaola *et al*., 2006). To assess contaminations in the fractions, the protein extracts were also challenged with antibodies against SurA and OmpA chosen as reporters of periplasmic and membrane proteins, respectively (Sklar *et al.*, 2007, Smith *et al.*, 2007). As shown in Figure 7, PhoN2 was found to be almost exclusively associated with the periplasmic fraction of bacteria grown at 37°C, in the presence or not of the Congo red dye. Accordingly, SurA and OmpA were found to be almost exclusively associated with the periplasmic and membrane fractions, respectively. As expected, *phoN2* expression was repressed when bacteria were grown at the non-permissive temperature of 30°C (Le Gall *et al.*, 2005; Santapaola *et al.*, 2006).

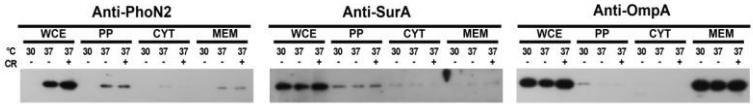

Fig. 7. PhoN2 accumulates in the periplasmic compartment of *S.flexneri*. Whole cell extract (WCE), membrane, cytosolic and periplasmic bacterial fractions of *S. flexneri* strain M90T were prepared from equal numbers of exponentially-grown bacteria. Bacteria were cultured at 30 and 37°C, and at 37°C in presence of CR, as described in Materials and Methods. Cell fractions were separated on a 12,5% SDS-PAGE. Following transfer of proteins to PVDF membrane, membranes were probed with anti-PhoN2 antibody and with anti-SurA, and anti-OmpA antibodies chosen as reporters of periplasmic and membrane proteins, respectively.

To trace PhoN2 within bacterial cells we constructed strain HNDHA10 by allelic exchange (Uzzau *et al*., 2001). Strain HNDHA10 is a derivative of the wild-type strain M90T carrying a C-terminal HA-tagged *phoN2* gene (*phoN2*::HA) (Table 1). In this strain, the expression of the fused gene is under the control of its native promoter. The introduction of the HA-tag did not influence the delivery of PhoN2-HA into the periplasm space since PhoN2-HA was predominantly detected within the periplasmic compartment (data not show). Taken together, these results clearly confirmed that PhoN2 is a periplasmic protein and indicated that the introduction of a HA-tag at its C-terminus did not influence its periplasmic delivery. Next, the intracellular localization of PhoN2-HA was determined by indirect immune-fluorescence experiments using HNDHA10 and anti-HA monoclonal antibody. Unexpectedly, these experiments showed that PhoN2-HA displayed foci that were polarly localized (Fig. 8A). Fluorescence spots were detected at both bacterial poles in 54.8±5.8% and at one pole in 39.3±4.4% of immunostained bacteria (n=1.350). Remarkably, in bacteria displaying PhoN2-HA foci at both poles, the intensity of the fluorescence signal was significantly more intense at the old pole (80.5% of immunostained bacteria). To get further insight on the polar localization of PhoN2, plasmid pHND10, a pBAD28-based recombinant plasmid carrying the *phoN2*::HA fusion under the control of an L-arabinose-inducible promoter, was generated and introduced into HND115, a Δ*phoN2* derivative of wild-type (Table 1) (Santapaola *et al.* 2006). Preliminarily, induction of *phoN2*::HA expression in HND115 carrying pHND10 was measured using a wide range of L-arabinose concentrations (from 0.002 to 0.2%). Real-Time PCR analysis showed that 0.016% of L-arabinose was the concentration that induced a level of *phoN2*::HA expression which more closely resembled that occurring in the wild-type strain grown in the presence of the Congo red dye, i.e. in conditions of MxiE-activated transcription (Fig. S1). Accordingly, unless otherwise indicated, 0.016% of L-arabinose was routinely used to induce *phoN2*::HA expression in the experiments described below. As expected, the *phoN2* mutant harboring pHND10, grown in the presence or not of 0.016% of L-arabinose, was as efficient as the wild-type strain in invading HeLa cell monolayers and, only when grown in the presence of L-arabinose, pHND10 complemented HND115 for plaque size and catalytic activity (data not shown) (Santapaola *et al*., 2006). Immuno-fluorescence experiments showed that, as HNDHA10, also the *phoN2* mutant harboring pHND10 displayed PhoN2-HA foci that were polarly localized both in exponentially-growing bacteria (91±6.5% of immunostained bacteria showed PhoN2-HA

at bacterial poles or at one pole) (Fig. 8B) and in bacteria within infected HeLa cells (Fig.8D). Moreover, the intensity of the fluorescence spots displayed by HND115 (pHND10) induced with 0.016% of L-arabinose were apparently comparable to that of HNDHA10 where the expression of the fused gene was under the control of its native promoter. PhoN2-HA foci were visualized only upon induction with L-arabinose (data not shown).Western blot analysis confirmed the periplasmic localization of the fused protein encoded by pHND10 even if bands of lower intensity and corresponding to PhoN2-HA were also evidenced in the cytoplasmic and membrane fractions (Fig. 11).

In order to to get further insight of the mechanism by which PhoN2 polarly localizes, pHND10 was introduced into the *E. coli* K-12 strain DH10b and polar fluorescent PhoN2-HA foci were visualized only when bacteria were grown in the presence of the inducer L-arabinose (Fig. 8C, and data not shown). These results indicate that the mechanism driving the polar localization of PhoN2 is conserved among *S. Flexner* and *E. coli.*

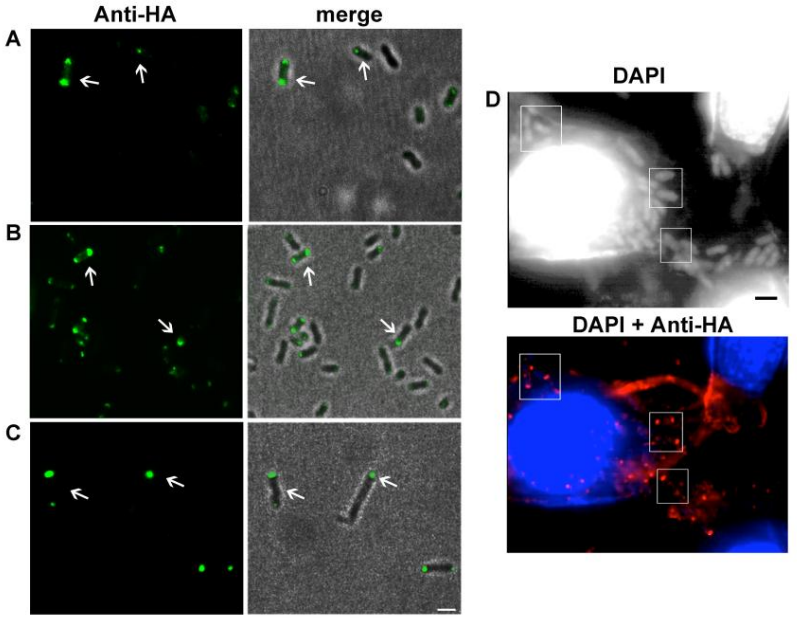

Fig. 8. PhoN2 localizes polarly in both exponentially-growing *S. flexneri* and *E. coli* K-12 strains. Indirect immunofluorescence experiments were carried out with HNDHA10 *phoN2*::HA, Panel A; HND115 (pHND10) cultured in the presence of 0.016% L-arabinose, Panel B and *E. coli* K-12 strain DH10b (pHND10) cultured in the presence of 0.016% L-arabinose, Panel C. PhoN2-HA was labelled with the anti-HA antibody (left column) and the fluorescence images were merged with phase contrast images (right column). Arrowheads indicate subpopulation of bacteria that display PhoN2-HA localized at bacterial poles. Bar = 2 µm. Panel D, Hela cells infected with HND115 (pHND10) strain, DAPI DNA staining (above) and DAPI and anti-HA merged fields (bottom). Boxs indicate subpopulation of bacteria that display PhoN2-HA localized at bacterial poles. Images are representative of three independent experiments.

PhoN2 localizes beneath the IcsA cap

IcsA is a *Shigella* surface-exposed protein that localizes at one bacterial pole (the old pole) from where it mediates ABM in host cells (Goldberg *et al.*, 1993, 1994). The basis of the unipolar localization of IcsA has been the subject of many studies and it represents one of the best-characterized model of polarity in enterobacteria (Fixen *et al.*, 2012). To verify a correlation between polar localization of IcsA and PhoN2 we performed immunofluorescence experiments marking both proteins with specific antibodies and taking into consideration only bacteria displaying PhoN2-HA localized at one bacterial pole. As shown in Fig. 9A, PhoN2 and IcsA were found at the same pole in the majority of stained cells (88.5±5.6%; n = 250 bacteria). These results clearly showed that periplasmic PhoN2-HA polarly localized at the level of the old bacterial pole, just beneath IcsA. This led us to hypothesize that some interaction between the two proteins might occur. To verify this hypothesis, we introduced pHND10 into the *icsA* mutant *S. flexneri* strain SC560 (Table 1). Since also in this strain PhoN2-HA displayed polarly localized foci (Fig. 9B), these results excluded that IcsA was required for the polar localization of PhoN2-HA.

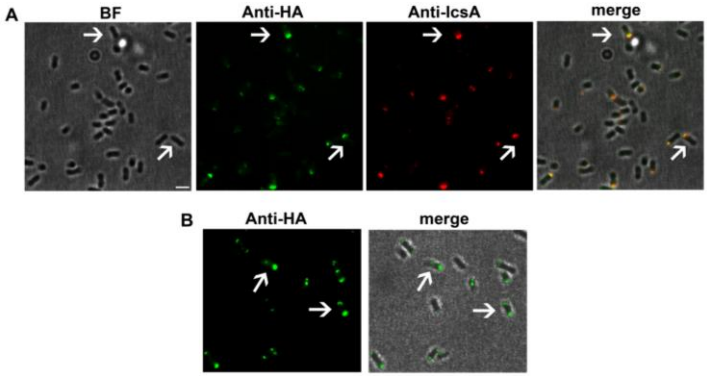

Fig. 9. PhoN2-HA localizes beneath the IcsA cap but its polar localization is independent by IcsA. Indirect immunofluorescence experiments were carried out with HNDHA10 *phoN2*::HA (Panel A) and SC560 (pHND10) (Panel B) cultured in the presence of 0.016% L-arabinose. Images are representative of phase contrast (BF), anti-HA (green), anti-IcsA (red), and the merged fields (A); anti-HA (green) and merged fields in B. Arrowheads indicate subpopulation of bacteria that displayed PhoN2-HA and IcsA localized at bacterial pole Bar= 2 µm.

Characterization of PhoN2 domains involved in its polar localization

Functional and in silico analysis of PhoN2 have led to the identification of three relevant domains: i) an N-terminal 23 amino acid leader sequence, which is processed during its passage across the cytoplasmic membrane; ii) an N-terminal domain encompassing an exposed PPPP sequence (^{43}PPPP^{46}); and iii) a C-terminal wide domain encompassing the putative ATP-diphosphohydrolase catalytic site. We have previously reported that while PhoN2 was required for proper *S. flexneri* cell-to-cell spread, apyrase catalytic activity was not (Santapaola *et al.*, 2006). To evaluate whether the catalytic activity of PhoN2 played a role in its polar localization, we introduced plasmid pHND19$_{R192P}$ [a pHND10-derivative plasmid carrying the R192P amino acid substitution of PhoN2 known to suppress apyrase activity (Sarli *et al*., 2005; Santapaola *et al*., 2006)] (Table 1) into the *phoN2* mutant strain HND115. As revealed by Western blot analysis, the R192P substituted protein was correctly delivered into the periplasmic compartment (Fig. 11). Since R192P substituted recombinant PhoN2-HA protein displayed polarly localized foci (Fig. 10B), this result clearly indicated that the deoxynucleotide triphosphate-hydrolyzing activity of PhoN2 is dispensable also for targeting PhoN2-HA to the bacterial poles. As expected, PhoN2-HA foci were detected only when bacteria were grown in the presence of L-arabinose (data not shown).

Next, a deletion of the fused gene which removed a DNA region encompassing the encoded PPPP motif (nucleotides 79-223) was generated in pHND10 (plasmid pHND11$_{\Delta 79\text{-}223}$) (Table 1). When plasmid pHND11$_{\Delta 79\text{-}223}$ was introduced into the *phoN2* mutant strain HND115, the Δ79-223 truncated HA-tagged protein, appeared as a diffuse signal (Fig. 10B). On average, in these experiments PhoN2-HA polarly localized foci were noticed in less than 3% of the bacterial population and in these cases the fluorescence signal was considerably reduced, compared to that displayed by parental pHND10. These results suggested that the polyproline domain could be important in the polar localization of PhoN2. Remarkably, pHND11$_{\Delta 79\text{-}223}$ failed to express apyrase activity (Fig. 10C), indicating that the polyproline domain could also play a role in catalysis.

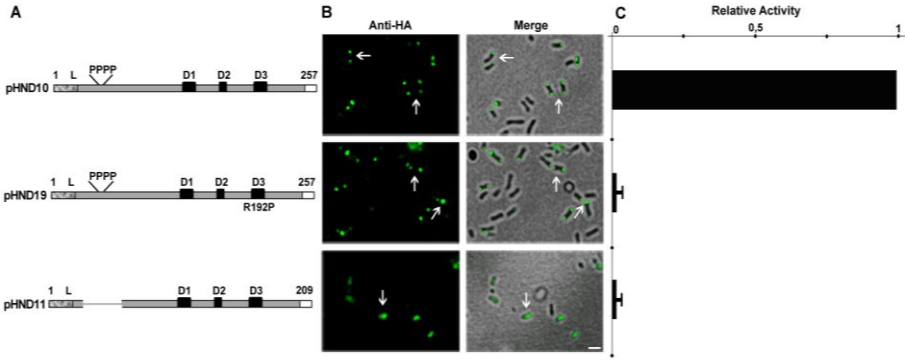

Fig.10 Characterization of PhoN2 domains involved in its polar localization and enzymatic activity

Panel A: in-frame deletion and amino acid substitution mutants of the HA-tagged *phoN2* gene. Amino acid residue 1 represents the first residue of the leader peptide (dotted box), while numbers on the right indicate the last residue of the tagged HA epitope (white box). The position of the PPPP motif is indicated. Conserved D1, D2 and D3 domains corresponding to the putative catalytic site of PhoN2 (black box) (Babu *et al*., 2002; Sarli *et al.*, 2005) and the substitution R192P, which inactivates apyrase activity, are indicated. Panel B: fluorescence microscopy, recombinant proteins were labeled with the anti-HA antibody (green) and fluorescence and phase contrast images were merged. Arrowheads indicate subpopulation of bacteria that display PhoN2-HA localized at bacterial poles. Panel C: ATP-hydrolysing activity of each recombinant protein calculated in comparison to the wild type protein. Bars represent the means of enzymatic activity of three independent experiments. Data are expressed as arbitrary units. Images are representative. Bar = 2 µm.

Site-directed mutagenesis were performed in order evaluate the role of the PPPP motif in the polar localization of PhoN2. To this end, a series of amino acid substitution within the PhoN2-HA PPPP motif carried by plasmid pHND10 were generated (see Materials and Methods for details). Four different derivatives of PhoN2-HA, carrying amino acid substitutions (P to S) of each of the P residues of the PPPP sequence, were generated and introduced separately into the *phoN2* mutant strain HND115. L-arabinose-

induced HND115 carrying plasmids pHND23$_{SPPP}$, pHND14$_{PSPP}$, pHND15$_{PPSP}$, and pHND16$_{PPPS}$ (Table 1), were assayed for PhoN2 polar localization, periplasmic delivery and for their ability to complement apyrase activity. As shown in Figure 11B, P to S substituted recombinant PhoN2-HA proteins encoded by pHND23$_{SPPP}$, pHND14$_{PSPP}$ and pHND15$_{PPSP}$ were correctly delivered into the periplasmic compartment, although Western blot analysis showed that that encoded by pHND15$_{PPSP}$ displayed a lower level of expression compared to the other two constructs (Fig. 11B). On the other hand, pHND16$_{PPPS}$, which also showed low levels of PhoN2-HA expression (Fig. 11B), was detectable only in the cytosolic fraction (Fig. 11B). Moreover, while pHND23$_{SPPP}$, pHND14$_{PSPP}$ and pHND15$_{PPSP}$ complemented HND115 for apyrase activity, (pHND15$_{PPSP}$ at a lower-extent, compared to pHND10), pHND16$_{PPPS}$ failed to complement (Fig. 11D). When the polar localization of the PhoN2-HA was analyzed (Fig. 11), substitution of the first (pHND23$_{SPPP}$) and second (pHND14$_{PSPP}$) proline residues apparently did not influence the polar localization of PhoN2-HA recombinant proteins (respectively 92.8±5.6% and 94.1±6.1% of the cells displayed PhoN2-HA polarly-localized foci). On the other hand, substitution of the third proline residue (pHND15$_{PPSP}$) induced a significant reduction of the percent of bacteria presenting polarly localized PhoN2-HA foci (about 57.7±4.9 of fluorescent bacteria showed polar fluorescence spots while 43.4±2.9% of bacteria showed a diffuse signal; *P* values < 0.05) (Fig. 11C). Remarkably, no fluorescence signals or apyrase activity were observed when HND115 was complemented with plasmid pHND16$_{PPPS}$.

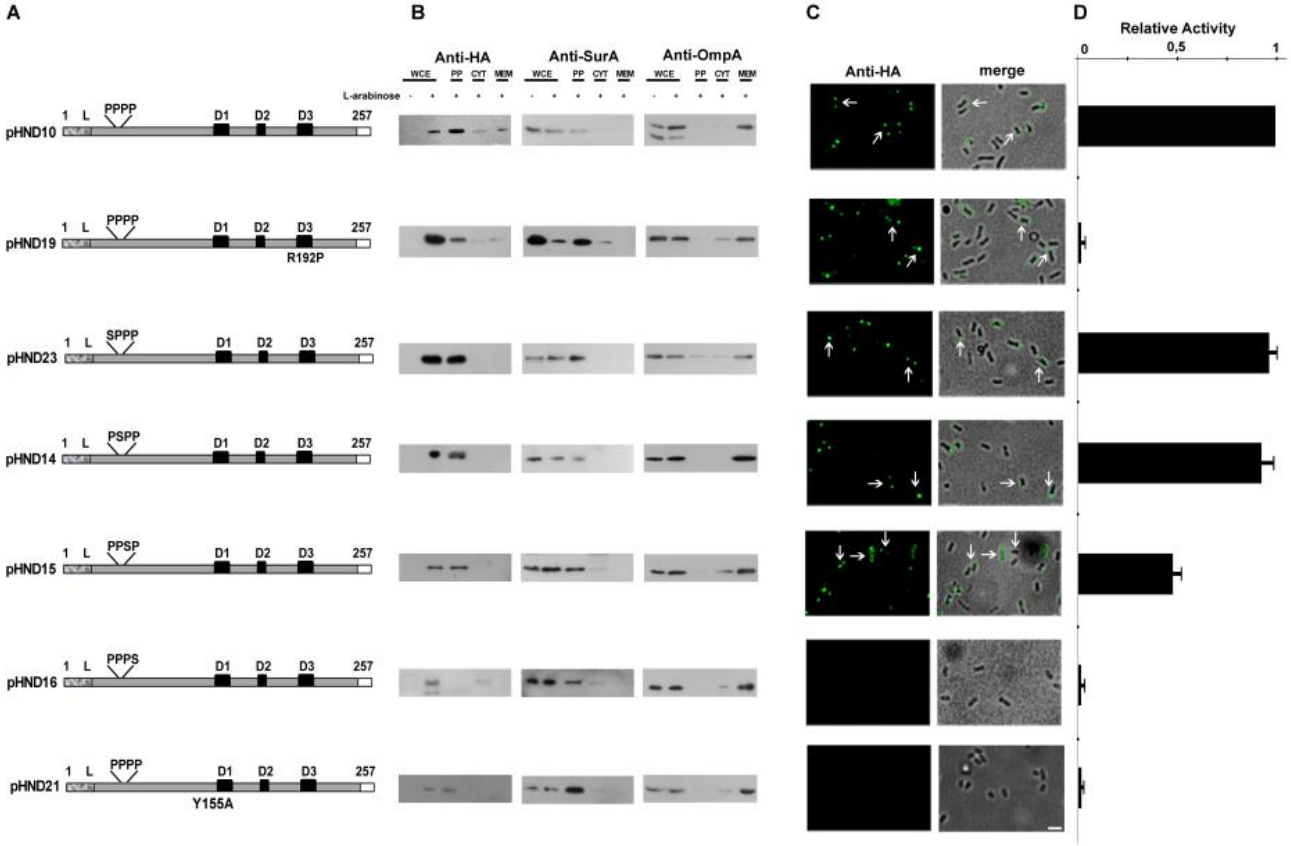
A
B
C
D
Anti-HA
Anti-SurA
Anti-OmpA
WCE
PP
CYT
MEM
L-arabinose
pHND10
pHND19
pHND23
pHND14
pHND15
pHND16
pHND21
1
L
PPPP
SPPP
PSPP
PPSP
PPPS
D1
D2
D3
257
R192P
Y155A
Anti-HA
merge
Relative Activity
0
0,5
1

Figure 11

Fig. 11. Characterization of the role of the PhoN2 PPPP motif and of amino acid residue Y155 in its periplasmic delivery, polar localization and enzymatic activity. Panel A: description of specific amino acid substitutions introduced into PhoN2-HA. Amino acid residue 1 represents the first residue of the leader peptide (dotted box), while numbers on the right indicate the last residue of the tagged HA epitope (white box). The position of the PPPP motif is indicated. The conserved D1, D2 and D3 domains (black box) corresponding to the putative catalytic site of PhoN2 (Babu *et al*., 2002; Sarli *et al.*, 2005) and the substitutions Y155A and R192P. Panel B: Whole cell extract (WCE), membrane, cytosolic and periplasmic bacterial fractions from equal numbers of exponentially-growing bacteria, cultured at 37°C, with 0.016% L-arabinose. Cell fractions were separated on a 12.5% SDS-PAGE. Following transfer PVDF membranes were probed with anti-PhoN2, anti-SurA and anti-OmpA antibodies. Panel C: fluorescence microscopy, recombinant proteins were labeled with anti-HA antibody (green) and fluorescence and phase contrast images were merged. Arrowheads indicate subpopulation of bacteria that display PhoN2-HA localized at bacterial poles Panel D: ATP-hydrolysing activity of each recombinant protein calculated in comparison to the wild type protein. Bars represent the means of enzymatic activity of three independent experiments. Data are expressed as arbitrary units. Images are representative. Bar= 2 µm.

The PPPP motif controls PhoN2 stability

The finding that PhoN2-HA encoded by pHND15$_{PPSP}$ and pHND16$_{PPPS}$ were expressed at lower levels, compared to that of pHND10, pHND23$_{SPPP}$, pHND14$_{PSPP}$ and pHND19$_{R192P}$ led us to consider whether the amino acid substitution of the third and fourth proline residues might have affected PhoN2 stability. To verify this hypothesis, the intracellular stability of PhoN2-HA carrying the different amino acid substitutions was monitored after protein synthesis had been inhibited by the addition of 100 µg/ml of spectinomycin. Samples were removed at different time points and whole cell extracts were immunodetected by Western blot. Quantitative measurements were carried out to estimate the half-lives of each recombinant proteins. As seen in Figure 12, the PhoN2-HA proteins encoded by L-arabinose-induced *phoN2* mutant carrying pHND10 (control), pHND23$_{SPPP}$, pHND14$_{PSPP}$ and pHND19$_{R192P}$ were stable throughout the duration of the experiment (half-lives of 276, 180, 265 and 270 min, respectively), while pHND15$_{PPSP}$, and pHND16$_{PPPS}$ displayed an high degree of protein instability already 30 min after protein synthesis had been inhibited (Fig. 12). We calculated half-lives of 28 and 5 min for proteins encoded by pHND15$_{PPSP}$, and pHND16$_{PPPS}$, respectively (Fig. 12). These results clearly showed that P to S substitutions of the third and of the fourth proline residues dramatically affected PhoN2 stability.

Next, to test if some specific protease was responsible for the degradation of these recombinant protein, we examined the level of PhoN2-HA encoded amino acid substituted proteins in different genetic backgrounds. Noteworthy, no significant difference in the steady-state levels of PhoN2-HA was noticed when recombinant plasmids were introduced into the *E. coli* K-12 strain DH10b (Fig. 5A), while high levels of PhoN2 instability were detected when pHND15$_{PPSP}$, and pHND16$_{PPPS}$ were introduced into strain BS176, a virulence plasmid-cured derivative of the *S. flexneri* strain M90T (Table 1) (Fig. 5B). These results clearly indicated that the structural gene(s) encoding the protease(s) involved in PhoN2-HA protein degradation are *S. flexneri*-specific and excluded that were encoded by genes localized on the virulence plasmid of *S. flexneri* strain M90T.

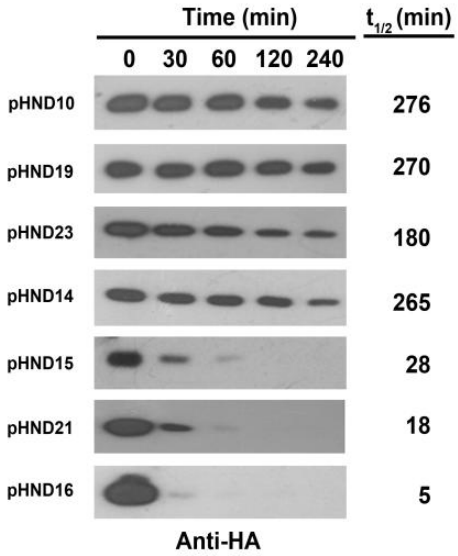

Fig. 12. Assessment of PhoN2 stability. HND115 carrying the indicated plasmids were grown to the mid-exponential phase, in the presence of 0.2% L-arabinose, and protein synthesis was inhibited by addition of Sp (100 μg ml^{-1}). Equal amount of bacteria were removed at 0, 30, 60, 120 and 240 min after Sp was added and re-suspended in 1 × Laemmli buffer. Protein extract were subjected to Western blot analysis. Densitometric analysis (ImageJ software) of each band was performed and half-lives ($t_{1/2}$ min) calculated for each recombinant protein. Images are representative.

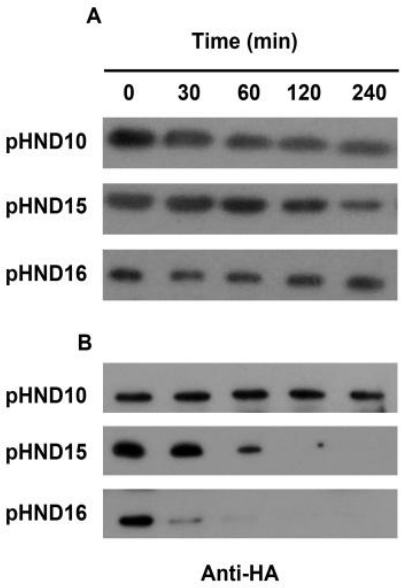

Fig. 13. A *Shigella* specific protease degrades PhoN2 mutant derivatives. Panel A: *E. coli* K-12 strain DH10b complemented with pHND10$_{PPPP}$, pHND15$_{PPSP}$, and pHND16$_{PPPS}$ cultured with 0.2% L-arabinose. Panel B: virulence plasmid-cured derivative of the *S. flexneri* strain BS176 complemented with pHND10$_{PPPP}$, pHND15$_{PPSP}$, and pHND16$_{PPPS}$ cultured with 0.2% L-ara. Bacteria were grown to the mid-exponential phase and protein synthesis was inhibited by the addition of Sp (100 μg ml^{-1}). Equal amount of bacteria were removed at 0, 30, 60, 120 and 240 min and re-suspended in 1 × Laemmli buffer. Protein extract were subjected to Western blot analysis. Images are representative.

The polyproline PPPP motif indirectly influences *S. flexneri* virulence

Previous work has shown that deletion of the *phoN2* gene led to altered actin comet tails and consequently to inefficient cell-to cell spreading and to a small plaque phenotype (Santapaola *et al*., 2006). The central bacterial mediator of actin based motility in *S. flexneri* is IcsA (Schoeder and Hilbi, 2008). Immunofluorescence experiments indicated that PhoN2 influenced IcsA exposition since, compared to the wild-type strain, the *phoN2* mutant strain HND115 displayed a significant reduction of IcsA exposition. This reduction was due to the lack of PhoN2, since complementation with pHND10 restored almost parental IcsA caps (Fig. 14), only when bacteria were supplemented with L-arabinose (approximately 78.6±7.8% of immunostained bacteria showed proper IcsA caps). These results indicated that PhoN2 is involved in the complex process of correct export and exposition of IcsA on *S. flexneri* bacterial surface. pHND23$_{SPPP}$, pHND14$_{PSPP}$, pHND15$_{PPSP}$ and pHND19$_{R192P}$ were also able to positively complement, at almost parental level, IcsA exposition, while pHND16$_{PPPS}$, likely because the high level of instability of the encoded PhoN2-HA substituted protein (Fig. 12), did not. Overall, these results showed that apyrase activity is not required for proper IcsA exposition and indicated that the PPPP motif, by influencing PhoN2 protein stability, is at least indirectly involved in the virulence of *S. flexneri.*

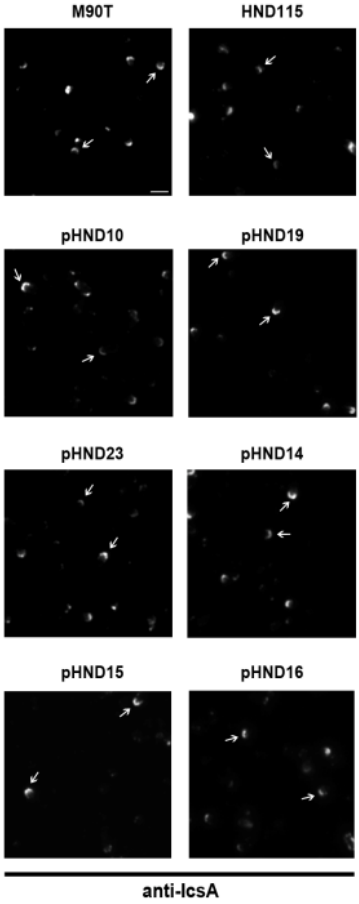

Fig.14. Fluorescence microscopy of IcsA. Parental strain M90T, HND115 and HND115 complemented with recombinant plasmids pHND10$_{PPPP}$, pHND23$_{SPPP}$, pHND14$_{PSPP}$, pHND15$_{PPSP}$, pHND16$_{PPPS}$, and pHND19$_{R192P}$. Were cultured in the presence of 0.016% L-arabinose. IcsA was detected in exponentially-grown bacteria, fixed with paraformaldehyde and labeled with polyclonal anti-IcsA antibody. The arrowheads indicate subpopulations of IcsA-labeled bacteria. Bar = 2 μm.

The poly-proline region is necessary for PhoN2 3D structure

As outlined in the Introduction section, PhoN2 belongs to the family of the class A of the non-specific bacterial acid phosphatases (A-NSAPs) a group of phosphatases highly diffused among Gram-negative bacteria (Rossolini *et al.*,1998). Among the relevant characteristics of this group of enzymes there is the presence of an N-terminal PPPP motif which was found to be highly conserved among all A-NSAPs analysed so far. While no data are available for PhoN2, it has been recently reported that the invariant residue Tyr-154 (Tyr-155 in PhoN2) by binding to the distal Pro-40 residue of the PPPP motif of PhoN (an A-NSAP encoded by *Salmonella* Typhimurium) stabilizes the loop harbouring the active site residues (Fig. 15) (Ishikawa *et al.*, 2000, Babu *et al.*, 2002, Makde *et al.*, 2007).

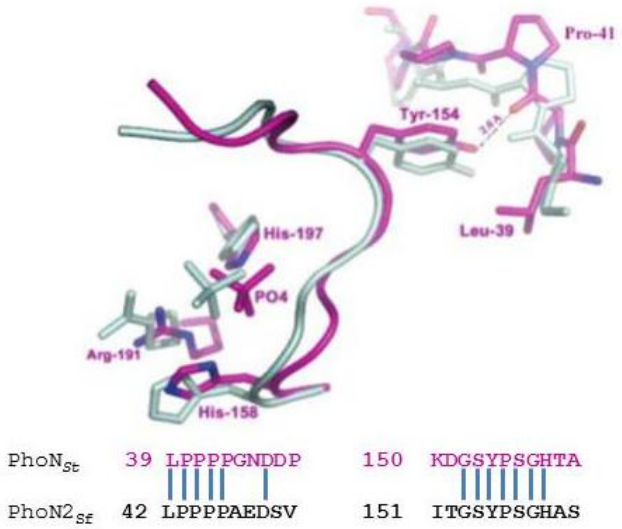

Fig. 15. Structurally conserved domains between PhoN of *Salmonella* Typhimurium and PhoN2 of *S. flexneri*. The loop harbouring active site residues (^{154}YPSGH^{158}) in PhoN from *S. typhimurium* (PhoN$_{St}$) is stabilized by the interaction between the highly conserved Tyr-154 residue and the distal ^{40}PPPP^{43} motif (shown in magenta). The sequence of Pho$_{St}$ in those critical motifs was aligned with PhoN2 from *S. flexneri* (PhoN2$_{Sf}$) to highlight highly conserved residues between primary sequences. Adapted from Makde et al., 2006.

On this basis, it was conceivable to hypothesize that the Tyr-155 residue of PhoN2 could exert a crucial structural role in protein conformational stability. To unravel this point, we generated pHN21$_{Y155A}$, a recombinant plasmid encoding the PhoN2-HA Y155A substitution (Table 1) (see Fig. 11 legend for details). pHN21$_{Y155A}$ was introduced into HND115 and stability of the substituted recombinant protein was evaluated by Western blot, after protein synthesis has been inhibited by the addiction of 100 µg/ml of spectinomycin, as described above. As shown in Figure 12, the substituted protein encoded by pHND21$_{Y155A}$ displayed a high degree of protein instability already 30 min after protein synthesis had been inhibited (half-live of 18 min). These results clearly showed that Tyr-155 along with the PPPP motif play a critical role in conformational stability of PhoN2 and indeed that the conformational stability is a key determinant of the proteolytic susceptibility of this protein. Interestingly, the inactivation of the catalytic domain does not influence the stability of the protein (pHND19$_{R192P}$: half-live of 270 min).
Finally, the influence of the Y155A substitution on the expression of apyrase activity and on the polar localization of PhoN2 was also evaluated. Accordingly to the results obtained with the highly unstable PhoN2-HA recombinant protein encoded by pHND16$_{PPPS}$, pHN21$_{Y155A}$ failed to complement HND115 for apyrase activity and no polar PhoN2 foci were detected in immune-fluorescence experiments (no fluorescence signals were observed) (Fig. 11), indicating that proper PhoN2 folding is required for the polar localization of this protein. Taken together these results clearly indicated that residue Tyr-155, by regulating protein stability, positively influences apyrase activity and the ability of PhoN2 to localize at the old bacterial pole of *S. flexneri*.

PhoN2 binds to the OM protein A (OmpA)

The localization of PhoN2 at the old bacterial pole raises the possibility that it might interact with bacterial protein(s) which assist PhoN2 in the accumulation at polar bacterial sites. To find and to characterize these specific protein(s), co-purification experiments were conducted with C-terminal 3xFLAG- or 6-His-tagged PhoN2, using affinity chromatography resins. Bound resins, challenged with a clear lysate of the wild-type strain, failed to detect any interaction partner (data not shown). Interaction partners were then searched by the two-hybrid technique in yeast. By using pGBKT7/*phoN2* as bait, the cDNA library of the wild-type strain fused in frame to the coding sequence of the GAL4-activating domain of plasmid

pGADT7-Rec (Table 1) was screened, as described in Materials and Methods. *Saccharomyces cerevisiae* AH109 competent cells were simultaneously transformed with the bait plasmid and the prey plasmid library and spread on selective plates. Plasmid DNA preparations of 16 independent transformants grown on minimal medium agar plates lacking leucine, tryptophan, histidine and adenine and expressing high-level of α-galactosidase, were used to transform *E. coli* DH10b competent cells selecting for kanamycin-resistance. The DNA inserts carried by independent prey plasmid DNA preparations were sequenced. Remarkably, the great majority of proteins encoded by the prey plasmids (13 out of the 16 examined) corresponded to the C-terminal domain of OmpA (Table 3). All OmpA inserts encompassed a common region composed of residues 189-273. The 189-273 residues represent the C-terminal domain of OmpA known to be exposed into the bacterial periplasm when the protein is in the eight-stranded β-barrel conformation (Koebnik and Kramer, 1995). These results were highly indicative of a PhoN2-OmpA interaction involving the periplasmic-exposed C-terminal domain of OmpA. As stated above, this interaction was not detected in co-purification experiments, most probably because the soluble form of OmpA was either not present in the bacterial clear lysate or not sufficient to be visualized by Comassie staining.

The sequence of the inserts of the three remaining prey plasmids (Table 3) encompassed amino acid residues of three different cytosolic *S. flexneri* proteins, namely Adh, AspRS and EF-2. The inserts encoded by these three plasmids were not analyzed further.

Table 3. Preys selected by the PhoN2 bait.

Prey	Start[a]	End[a]	Number of clones[b]	Common region[c]
OmpA (348 aa)	189	276	5	189-273
	185	304	2	
	43	275	2	
	188	299	1	
	51	273	1	
	72	277	1	
	186	284	1	
Adh (336 aa)	129	218	1	
AspRS (590 aa)	358	472	1	
EF-2 (665 aa)	114	264	1	

[a]Aminoacid coordinates, with respect to the sequence of the native proteins, of the first and last residue encoded by the insert in each prey plasmid.
[b]Number of independent clones containing identical prey fragments.
[c]Coordinates of the common region carried by all preys corresponding to the same protein.

In vivo *cross-linking experiments*

To confirm the interaction between PhoN2 and OmpA, *in vivo* cross-linking experiments were conducted using formaldehyde (Fig. 16). Cross-linking was performed with the *phoN2* mutant strain HND115 carrying pHND10, grown in the presence (Fig. 16 B and D) or not (Fig. 16 A and C) of 0.016% of L-arabinose (see Materials and Methods for details). Total protein extracts were separated by SDS-PAGE and analyzed by Western blot using monoclonal anti-HA (Fig. 7A and B) and polyclonal anti-OmpA antibodies (Fig. 16 C and D). Western blot of bacterial extracts, denatured at 95°C in Laemmli buffer prior to electrophoresis, detected PhoN2-HA (Fig. 16 B, lanes 4 and 6) and unfolded OmpA (Fig. 16 C and D, lanes 7, 9, 10 and 12) of the expected molecular size (28 and 35 kDa, respectively), while in samples heated at 37°C OmpA migrates as a folded 30 kDa protein (Fig. 16 C and D, lanes 8 and 11) (Schweizer *et al.*, 1978). On the other hand, extracts of formaldehyde-treated bacteria, expressing both PhoN2-HA and OmpA, generated an additional molecular species when samples were heated at 37°C (Fig. 16 B and D, lanes 5 and 11). This new molecular species migrated with an apparent mass of 63 kDa, consistent with the molecular size corresponding to the sum of mature PhoN2-HA and OmpA.

The intensity of the new band was strongly reduced when heated at 95°C (Fig. 16 B and D, lanes 6 and 12). As expected, no PhoN2-HA signal was detected in the absence of L-arabinose (Fig. 7A, lanes 1 to 3). Taken together these results are consistent with the finding of a PhoN2-OmpA interaction.

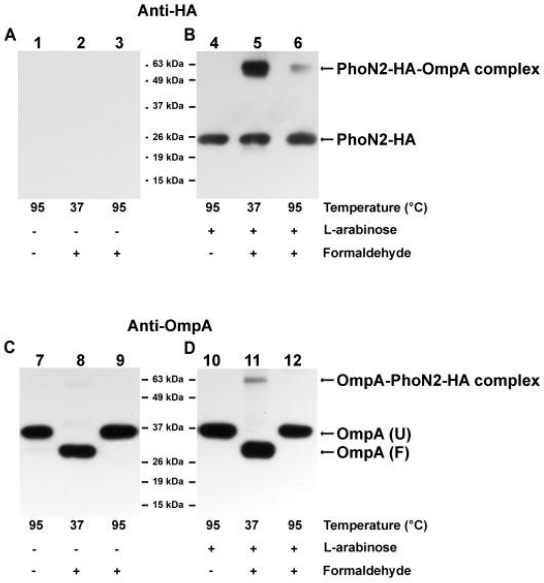

Fig. 16. ***In vivo*** **cross-linking experiments.** Cross-linking of HND115 (pHND10) was achieved by treating bacteria with formaldehyde to a final concentration of 1%, as described in Materials and Methods. Samples were suspended in Laemmli buffer and either heated at 37°C for 10 min to maintain cross-links or at 95°C for 20 min to break cross-links. Equal amounts of proteins were analyzed by Western blot. A protein molecular weight marker (Pierce) was used to determine the molecular weight of proteins. Immunoblot was carried out with monoclonal anti-HA (Panels A and B) or polyclonal anti-OmpA antibodies (Panels C and D). Expression of PhoN2 was achieved by growing bacteria in the presence of 0.016% of L-arabinose. Panels A and C, bacteria not induced with L-arabinose; Panels B and D, L-arabinose induced bacteria. OmpA (U), unfolded OmpA; OmpA (F), folded OmpA (Schweizer *et al*., 1978). Representative images of Western blot of cross-linking experiments.

Effect of OmpA on the polar localization of PhoN2

To investigate whether OmpA was involved in the polar localization of PhoN2, the *ompA* mutation of the *E. coli* strain JW0940 was P1 transducted into the *phoN2* mutant strain HND115, thus generating derivative strain HND93 (Table 1). Remarkably, HND93, when complemented with pHND10 and only when grown in the presence of 0.016% of L-arabinose, displayed polarly localized PhoN2-HA (Fig. 17**A**) in the great majority of immunostained cells (92.3±5.2% of cells displayed polarly localized PhoN2-HA and, of these, 40.3±4.4% displayed PhoN2-HA localized only at the old bacterial pole). Next, pHND10 was introduced into OmpA-proficient and –deficient *E. coli* K-12 strains ME9062 and JW0940 Δ*ompA* (Table 1) to determine PhoN2-HA localization in a K-12 genetic background. Again, both *E. coli* strains displayed PhoN2-HA polarly localized (Fig. 17B and C) at rather the same extent displayed by strain HND93 (pHND10) (data not shown). Thus, in spite of its specific interaction with PhoN2, these results excluded that OmpA was required for the polar localization of PhoN2.

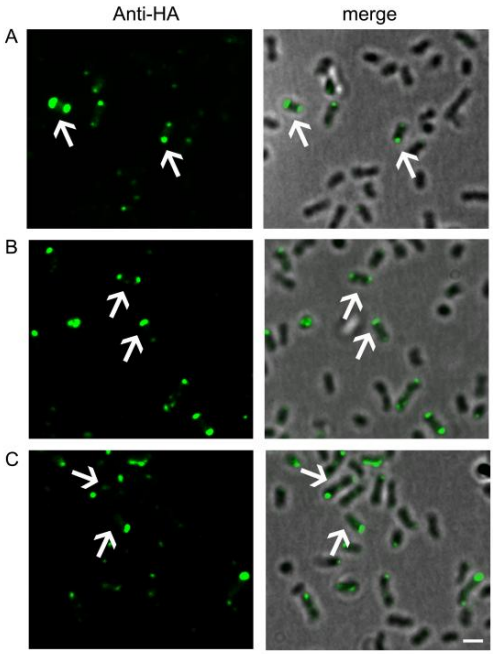

Fig. 17. PhoN2 localizes polarly in a *S. flexneri ompA* mutant and in both OmpA-proficient and –deficient *E. coli* K-12 strains. Indirect immunofluorescence experiments were carried out with HND93 (pHND10), Panel A; ME9062 (pHND10), Panel B and JW0940 (pHND10), Panel C. All strains were cultured in the presence of 0.016% L-arabinose. PhoN2-HA was labeled with the anti-HA antibody (left column) and the fluorescence images were merged with phase contrast images (right column). Arrowheads indicate subpopulation of bacteria that display PhoN2-HA localized at bacterial poles. Bar = 2 µm. Images are representative.

Interaction between PhoN2 and OmpA: a computational model

Analysis of the PhoN2 structural model evidenced the presence of a long unstructured N-terminal region folding onto the protein core. The interaction of this region with the remaining part of PhoN2 structure is

mainly mediated by the ^{43}PPPP^{46} polyproline motif. The observation that OmpA displays a similar polyproline motif (^{183}PAPAP^{187}), located within the periplasmic C-terminal domain, led us to hypothesize that OmpA could interact with PhoN2 by displacement of the PhoN2 N-terminal region and interaction of the ^{183}PAPAP^{187} motif with PhoN2 protein core. This hypothesis was first analysed by removing the N-terminal region from PhoN2 structural model and manually docking OmpA ^{183}PAPAP^{187} motif onto PhoN2 protein core. This analysis evidenced the compatibility of the OmpA ^{183}PAPAP^{187} motif with the PhoN2 protein core, suggesting that OmpA ^{183}PAPAP^{187} motif might substitute the PhoN2 ^{43}PPPP^{46} motif, by binding to residues Y155, thereby leading to the stabilization of PhoN2 in the complex. To test this prediction, we performed *in vivo* cross-linking experiments, as outlined above. To this purpose, using pACYC184-carrying the *ompA* gene cloned together with its natural promoter (Table 1), we first generated specific point mutations in order to express a recombinant OmpA protein presenting P to A substitutions of all proline residues within the OmpA ^{183}PAPAP^{187} motif (generating an ^{183}AAAAA^{187} motif). According to our model, we expected that the P to A substitutions should totally destroy the rigidity of the encompassed region and abrogate the hydrophobic interactions within prolines residues of the PhoN2 PPPP motif. To evaluate this prediction, the *ompA phoN2* mutant strain HND93, was co-transformed with plasmids pHND10 and pAAAOmpA, a pACYC184-based recombinant plasmid carrying the mutated recombinant *ompA* sequence encoding the ^{183}AAAAA^{187} motif under the control of its endogenous promoter (Table 1) and subjected to cross-linking experiments. As a positive control strain HND93 co-transformed with plasmids pHND10 and pOmpA was used (Table 1).

As shown in Figure 18, a protein complex migrating with an apparent mass of 63 kDa, corresponding to the sum of PhoN2-HA and OmpA, was displayed in formaldehyde-treated whole protein extracts of HND93 carrying pHND10 and pAAAOmpA (right panels) as well as in the control strain HND93 co-transformed with plasmids pHND10 and pOmpA (left panels). No signal corresponding to PhoN2-HA could be detected in bacteria not induced with L-arabinose (data not shown). These results led us to conclude that the ^{183}PAPAP^{187} motif is likely not involved in the PhoN2-OmpA interaction or that motifs other than the ^{183}PAPAP^{187} motif concurred in the interaction with PhoN2. Experiments based on the two-hybrid yeast assay methodology are in progress to definitively settle this point.

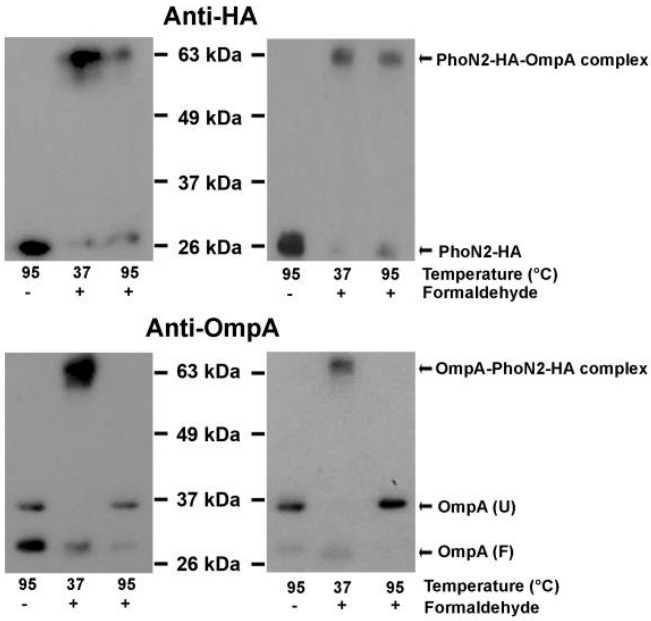

Fig. 18. The P to A substitutions within the OmpA ^{183}PAPAP^{187} motif do not abrogates the interaction between OmpA and PhoN2. Cross-linking of HND93 carrying pHND10 and pOmpA (left panels) and HND93 carrying pHND10 and pAAAOmpA) (right panels) was achieved by treating bacteria with formaldehyde, as described in Material and Methods. Samples were suspended in Laemmli buffer and either heated at 37°C for 10 min to maintain cross-links or at 95°C for 20 min to break cross-links. Equal amounts of proteins were analyzed by Western blot. A protein molecular weight marker (Pierce) was used to determine the molecular weight of proteins. Immunoblotting was carried out with monoclonal anti-HA or polyclonal anti-OmpA antibodies, as indicated. Expression of PhoN2 was achieved by growing bacteria in the presence of 0.016% of L-arabinose. OmpA (U), unfolded OmpA; OmpA (F), folded OmpA (Schweizer *et al*., 1978). Representative image of Western blot of cross-linking experiments.

Role of OmpA in the mechanism of pathogenicity of S. flexneri.

As outlined in the Introduction Section, OmpA is an outer membrane pleiotropic protein embedded in the bacterial OM as a β-barrel protein, highly conserved among Gram-negative bacteria (Krishnan and Prasadarao, 2012). It has been reported that OmpA plays a pivotal role in the structural integrity of the OM and that it has to be considered an important virulence factor of several human pathogens (Krishnan and Prasadarao, 2012; Smith et al., 2007, Reusch, 2012). Recently OmpA of *S. flexneri* 2a has been identified as a novel molecule coordinating the innate and adaptive immune responses, strongly indicating that OmpA may also represent a promising antigen in vaccine development (Pore *et al.*, 2009, Pore *et al.*, 2012). Since, in spite of its importance in the immune response of *S. flexneri*, to date no reports have documented the role of OmpA on the virulence of *S. flexneri*.

Construction of the *ompA* mutant strain HND92

To investigate the role of OmpA in *S. flexneri* virulence, a Δ*ompA* mutation carried by the *E. coli* K-12 strain JW0940 (Table 1) was introduced into the wild-type *S. flexneri* strain M90T by P1 transduction. The correct structure of tranductants was verified by DNA sequencing (see Material and Methods for details) and one of them, named HND92, was used in all experiments. HND92 was able to bind Congo red and did not present growth defects since, in LB medium, there was no difference between the optical density of HND92 and that of the wild-type strain (data not shown). Exploiting the known cross-reactivity between enterobacterial species (Hofstra *et al.*,1980), we used polyclonal rabbit anti-OmpA antibody, raised against the *E. coli* OmpA protein, to detect OmpA in *S. flexneri*. A band of the expected size of OmpA (35 kDa) was detected by Western blot of whole cell extracts of the wild-type strain, while no detectable band corresponding to OmpA was observed in HND92 (Fig. 19). Complementation of the *ompA* mutation with plasmid pOA, which carries the *ompA* gene and its promoter region cloned into the plasmid vector pACYC184 (Table 1), restored OmpA expression. Moreover, proper localization within the membrane fraction and folding of OmpA was also assayed. Native OmpA of *E. coli* is known to present typical heat-modifiable mobility of β-barrels in SDS-PAGE which are known to form a compact SDS-resistant structure at low-temperature (37°C) that unfolds upon heating at higher temperature (100°C) (Cock *et al.*, 1996, Sugawara *et al.*, 1996]. Indeed, both OmpA of *S. flexneri* and OmpA expressed by

recombinant plasmid pOA behaved as native *E. coli* OmpA, since both proteins were found to be strictly localized within the membrane fraction and presented the expected heat-variable mobility (Fig. 19 and data not shown). These results indicated that OmpA of *S. flexneri* presented the same relevant biological characteristics of OmpA of *E. coli*.

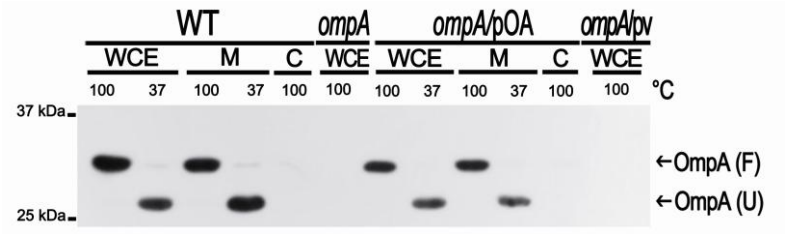

Fig. 19. Western blot analysis of OmpA expression. OmpA expression by the wild-type *S. flexneri* 5a strain M90T (WT), the *ompA* mutant (*ompA*), the *ompA* mutant complemented with plasmid pOA (*ompA*/pOA) and the *ompA* mutant complemented with the empty vector pACYC184 (*ompA*/pv) is shown. WCE, whole cell extract; M, crude membrane fraction; C, cytosolic and periplasmic fraction. Fractions were suspended in 1 × Laemmli buffer and heated at 37°C or at 100°C for 10 min before SDS-PAGE to evaluate the unfolded (U) and folded (F) forms of OmpA (38 Cock *et al.*, 1996, Sugawara *et al.*, 1996). PVDF filters were probed using an anti-OmpA polyclonal antiserum. The positions of U and F forms of OmpA are indicated by arrows at the right side. Size markers (kDa) are shown at the left side.

The *ompA* mutation does not affect IpaABCD secretion

To assess whether the *ompA* mutation affected the ability of *S. flexneri* to synthesize and secrete IpaABCD effector proteins, we compared IpaABCD synthesis and secretion in the wild-type strain M90T and in its *ompA* derivative mutant strain HND92 (Table 1). Exponentially-growing of wild-type and of HND92 were incubated in the presence of CR in order to activate the T3SS system (Santapaola *et al.*, 2006) (see Materials and Methods for details). SDS-PAGE analysis of Comassie brilliant blue staining of whole bacterial extracts and of concentrated culture supernatants indicated that neither the production nor the secretion of IpaABCD proteins were affected by the inactivation of the *ompA* gene (Fig. 20A).

Accordingly, immunoblot using anti-IpaB and anti-IpaC antibodies showed no difference in the expression and secretion of both proteins by both strains (Fig. 20B). These results clearly indicated that the HND92 has a functional T3SS system.

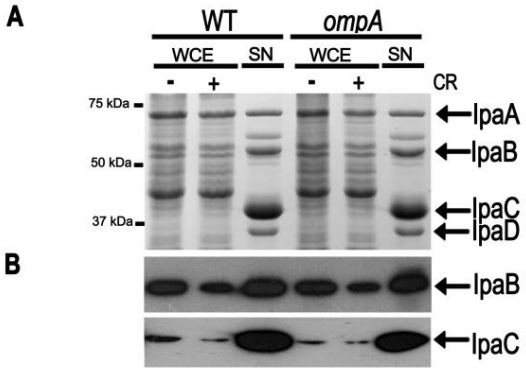

Fig. 20. The *ompA* mutation did not affect either production or secretion of IpaABCD proteins. Proteins present in WCEs and concentrated culture supernatants (SN) of the wild-type strain (WT) and of the *ompA* mutant (*ompA*), following exposure of bacteria to 7 μg ml^{-1} of Congo Red (CR), were stained with Comassie brilliant blue (A) or transferred to a PVDF membrane and probed using anti-IpaB and anti-IpaC antibodies (B). The positions and names of the various proteins are indicated at the right side. Size markers (kDa) are shown at the left side.

The *ompA* mutant presents an altered invasive phenotype

Next, the ability of the *ompA* mutant to invade and to multiply within semi-confluent HeLa cell monolayers was compared to that of wild-type. The *ompA* mutant was proficient both in host cell invasion and intracellular multiplication (Fig. 21). Interestingly, at 5 h post-infection HND92 displayed a reduced invasion phenotype. On average, we found that the number of HND92 bacteria in the cytoplasm was higher than that of wild-type (216 ± 22 and 158 ± 18 bacteria per infected HeLa cell, respectively). In contrast, whereas the percentage of cells infected by the wild-type strain was 82.1 ± 12.0%, the proportion of cells infected by HND92 was 46.2 ± 6.3% ($P \leq 0.05$). Moreover, at 3 h post-infection striking differences

regarding the intracellular bacterial distribution were observed in Giemsa stained monolayers (Fig. 21). While wild-type displayed the characteristic random distribution within the cytoplasm of HeLa cells, the *ompA* mutant showed a less randomly distributed behaviour with bacteria organized in parallel arrays and which seemed to be entrapped within the cell cytoplasm. This intra-cellular distribution was reminiscent of that of *mlaA*/*vacJ S. flexneri* mutants impaired in inter-cellular spread (Suzuki *et al.*, 1994), and significantly different to that shown by the *icsA* mutant strain SC560 (Table 1) which displayed bacteria growing in cluster in the cell cytoplasm (Fig. 21, insets). Moreover, random distribution of bacteria within the cytoplasm of HeLa cells was restored when the *ompA* mutant was complemented with plasmid pOA (Table 1), indicating that OmpA is required for normal distribution of *S. flexneri* in the cell cytoplasm. Noteworthy, differently from wild-type, protrusions were noticed only sporadically in HeLa cells infected with the *ompA* mutant. This finding prompted us to measure the frequency of protrusion formation. Assuming a relative arbitrary value of 100% for the number of protrusions (per infected HeLa cells) formed by the wild-type strain 1 h post-infection, under these conditions the *ompA* mutant scored about 6.9 ± 2.4%, while HND92/pOA displayed about 89.7 ± 6.9% ($P \leq 0{,}01$). These results clearly indicated that the lack of OmpA was responsible of the protrusion defect of the *ompA* mutant. Cytoplasmic entrapment of bacteria and the dramatic decrease in protrusion formation were highly suggestive of impaired actin-based motility (ABM).

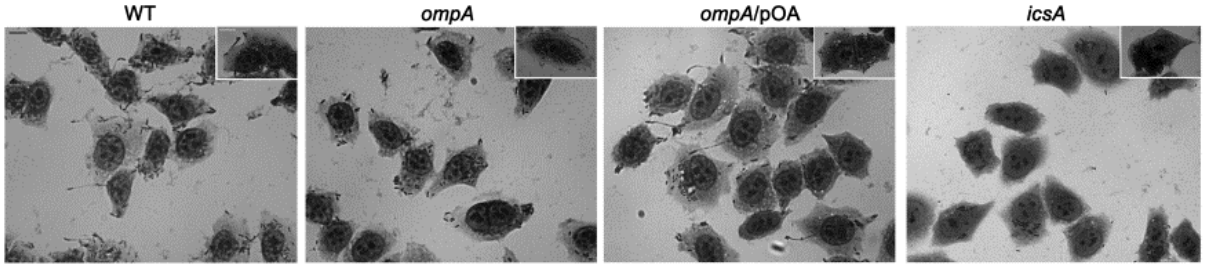

Fig. 21. The *ompA* mutant retained wild-type invasion efficiency. Semi-confluent HeLa cell monolayers were infected with the wild-type strain (WT), the *ompA* mutant (*ompA*), and the *ompA* mutant complemented with plasmid pOA (*ompA*/pOA), at a MOI of 20. Monolayers were fixed with methanol and Giemsa-stained for microscopic evaluation at 1 h and 3 h post-infection (insets). The *icsA* mutant SC560 strain was included as control (*icsA*). Representative images of at least four independent experiments are shown. Scale bar, 10 µm

Therefore, the ability of the *ompA* mutant to form F-actin comet tails and to plaque on HeLa cells was determined. As wild-type, the *ompA* mutant was found to be proficient in the formation of apparently normal F-actin comet tails (Fig. 22), as determined by measuring the frequency of bacteria presenting apparently normal actin tails per infected HeLa cell (22.2 ± 1.5% and 24.2 ± 2.7% for wild-type strain and the *ompA* mutant, respectively; $P \geq 0.5$). Unexpectedly, despite the formation of proper actin tails, the *ompA* mutant failed to plaque on confluent HeLa cell monolayers (Fig. 23), even when HeLa cells were infected at higher MOIs or extending the period of incubation (data not shown). The ability to produce plaques at almost wild-type level was rescued by complementing the *ompA* mutant with plasmid pOA (0.9-1.2 mm against 1.0-1.2 mm of wild-type, after 72 h of incubation) (Fig. 23), indicating that a functional OmpA protein is required and sufficient for the inter-cellular spread of *S. flexneri*.

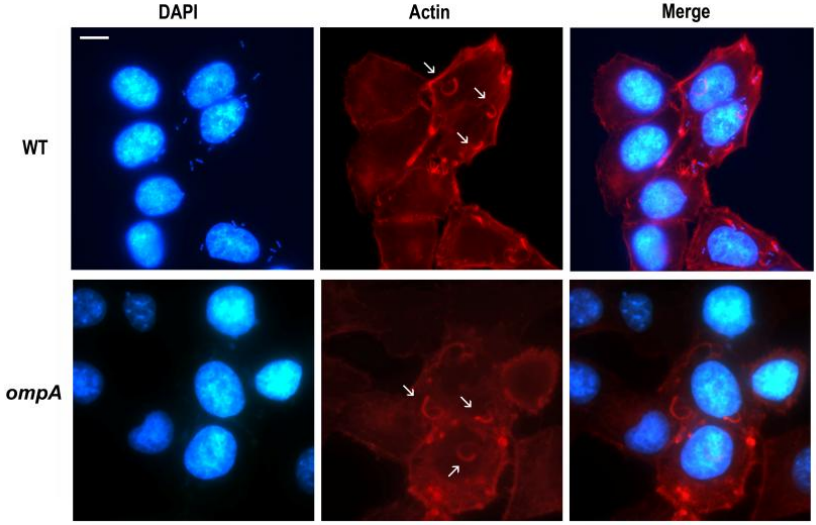

22. The *ompA* mutant retained the ability to form wild-type F-actin comet tails. Semi-confluent HeLa cell monolayers were infected with the wild-type strain (WT), the *ompA* mutant (*ompA*), and the *ompA* mutant complemented with plasmid pOA (*ompA*/pOA). Actin was stained with rhodamine-conjugated phalloidin (red). Nuclei and bacterial DNA were stained with DAPI (blue). Representative images of double immunofluorescent microscopy are shown. Arrows points representate bacteria exhibiting normal F-actin comet tail formation. Scale bar, 10 µm.

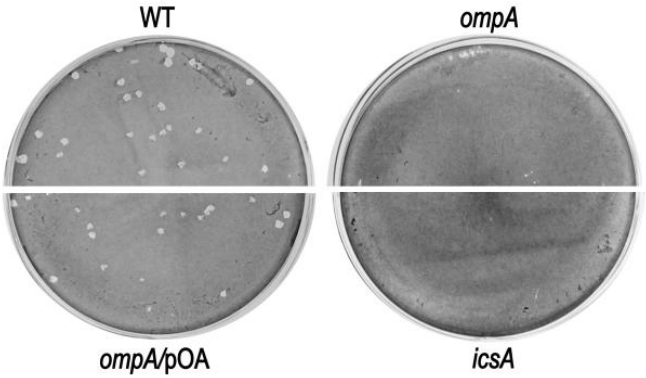

Fig. 23. The *S. flexneri ompA* mutant failed to plaque on HeLa cell monolayers. Confluent HeLa cell monolayers were infected with the wild-type strain (WT), the *ompA* mutant (*ompA*), and the *ompA* mutant complemented with plasmid pOA (*ompA*/pOA), at a MOI of 4. The *icsA* mutant SC560 strain (*icsA*) was included as a plaque negative control. Cells were Giemsa-stained and photographed 72 h post-infection. Images are representative.

Previous studies have reported that mutations of genes involved in the biosynthesis of the LPS of *S. flexneri* lead to the inability to plaque (Morona and Van Den Bosch, 2003, Van Den Bosch and Morona, 2003). To determine whether the lack of OmpA could have altered LPS biosynthesis, thus causing the inability of the *ompA* mutant to plaque, we first evaluated the sensitivity of the *ompA* mutant to the killing of normal human serum (NHS), since it has been reported that wild-type LPS of *S. flexneri* is required to confer resistance to NHS killing (Hong and Payne, 1997). To this end, mid-log cultures of the *ompA* mutant, of the wild-type strain and of the *E. coli* K-12 DH10b (used as a serum-sensitive control) were incubated for 2 h (30 min intervals) in the presence of 10% of NHS or with heat-inactivated normal human serum (HIS). The percent survival to killing of the *ompA* mutant was indistinguishable to that of the wild-type strain while, as expected, the *E. coli* DH10b strain was highly sensitive to NHS. There was a greater than 5 log difference between the CFUs of *E. coli* DH10b rescued after 30 min of incubation in 10% NHS and the CFUs of wild-type and the *ompA* mutant after 2 h of incubation (data not shown). Next, LPS preparations were prepared as described in Materials and Methods. Aliquots were subjected to SDS-13%-PAGE and visualized by

silver staining. Fig. 24 shows that the *ompA* mutant produced the typical LPS structure seen in the wild-type strain, thus definitively ruling out that the lack of OmpA might have altered LPS biosynthesis and that the inability to plaque of the *ompA* mutant was due to LPS alterations.

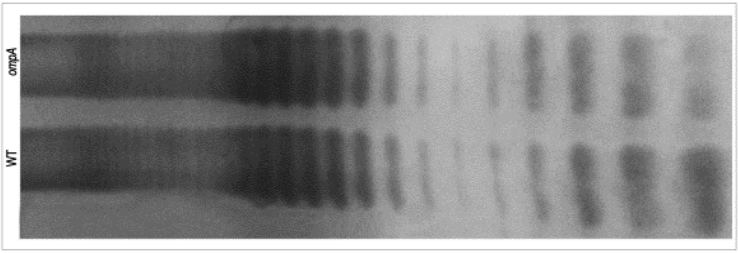

Fig. 24. LPS profiles of the wild-type strain (WT) and of the *ompA* mutant (*ompA*). LPS was extracted as described in Materials and Methods, resolved by SDS-13%PAGE and silver stained.

Polarly-localized IcsA is essential for ABM in *Shigella* (Bernardini *et al.*, 1989, Cossart, 2005). To study the influence of OmpA on IcsA surface exposition at the bacterial pole, indirect immunofluorescence experiments were conducted using a polyclonal IcsA antiserum. Differently from the typical polar IcsA caps displayed by the wild-type strain, the great majority of *ompA* immunostained bacteria showed IcsA exposed across the entire bacterial surface [90.0 ± 8.7% of the *ompA* mutant displayed IcsA diffused across the entire bacterial surface; 9.5 ± 2.2% displayed apparently normal IcsA caps and 0.5% produced polar IcsA caps smaller than wild-type strain, while 55.3 ± 8.2% of wild-type bacteria displayed typical normal IcsA caps, 26.2 ± 5.9% also displayed IcsA exposed at the old bacterial pole but the caps appeared smaller than typical IcsA caps, and 18.5 ± 3.7% displayed IcsA diffused across the entire bacterial surface ($P < 0.01$). Under these experimental conditions the percentage of immunostained bacteria were 26.5% for the *ompA* mutant (n=2950), and 31.3% for wild-type strain (n=2880) ($P > 0.5$)] (Fig. 25). Noteworthy, the majority (about 62.0 ± 7.8%) of the *ompA* mutant immunostained bacteria presented IcsA polar reinforcements (data not shown). pOA-complementation restored wild-type IcsA exposition (Fig. 25). Taken together, these results indicated that OmpA, while it is not required for the ability of *S. flexneri* to invade and multiply within host cells as well as to produce proper F-actin comet tails, it is absolutely required for protrusion formation, cell-to-cell spread and proper IcsA surface exposition.

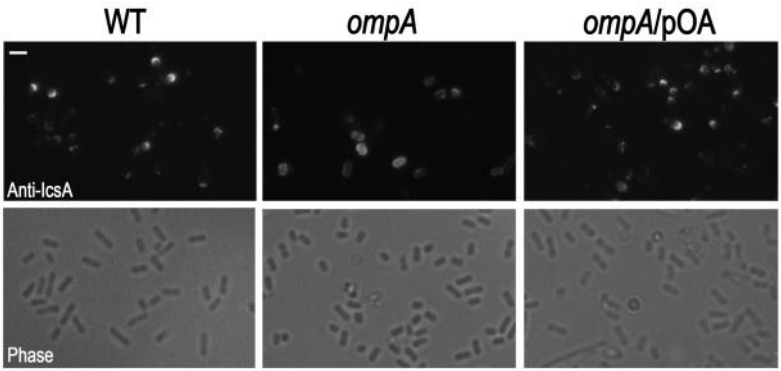

Fig. 25. The lack of OmpA altered exposition of IcsA at *S. flexneri* lateral bacterial surface. Exponentially-growing wild-type strain (WT), the *ompA* mutant (*ompA*), and the *ompA* mutant complemented with plasmid pOA (*ompA*/pOA) were analyzed by indirect immune-fluorescence using an anti-IcsA polyclonal antiserum. Representative images from at least three independent experiments are shown. Scale bar, 5 μm.

To determine whether OmpA contributed to the presentation of IcsA on the bacterial surface, as well as to the release of IcsA* (the IcsP-cleaved 95 kDa polypeptide) into culture supernatants (Egile *et al.*, 1997, Santapaola *et al.*, 2006, Wagner *et al.*, 2009), WCE and culture supernatants of the *ompA* mutant, of its pOA-complemented derivative strain and of wild-type were analyzed by Western blot. Unexpectedly, when compared to wild-type, the *ompA* mutant displayed significant reduced levels of IcsA (56.6 ± 4.8%; $P \leq 0.05$) and this reduced expression was due to the lack of OmpA since complementation with plasmid pOA increased these levels to 87.5 ± 5.3% (Fig. 26A). It has been recently reported that a fraction of the IcsP-mediated cleavage products of mature IcsA remains cell associated (ca-IcsA*) so that it can be detected in WCE (Wagner *et al.*, 2009). Densitometry analysis of WCE and of supernatant fractions revealed that wild-type, the *ompA* mutant and the pOA-complemented strain displayed similar amounts of IcsA* and of ca-IcsA* (Fig. 26A and B). These results indicated that the reduction of IcsA expression observed in the *ompA* mutant did not influence the levels of IcsP-cleaved IcsA* and ca-IcsA*.
The reduction of IcsA expression in the *ompA* mutant could be due either to reduced IcsA levels in the cell or to a reduction of the amount of IcsA detectable by antibody on the bacterial surface. To investigate these

possibilities, we first investigated whether the reduction of IcsA expression was due to reduced *icsA* transcription. Real Time PCR analysis (Tran *et al.*, 2011), conducted on cDNA preparations of wild-type and the *ompA* mutant, clearly indicated that the reduction of IcsA expression was not due to reduced transcription (data not shown). Furthermore, the amount of IcsA exposed at the surface of the *ompA* mutant and of the pOA-complemented derivative strain were determined and compared to that of wild-type by quantifying HRP enzymatic activity (Purdy *et al.*, 2007) as well as by immuno-dot blot experiments (see Materials and Methods for details). For each strain, the ratio of anti-IcsA-HRP enzymatic activity to anti-*Shigella* LPS signal was determined in order to normalize the IcsA-HRP signal to the number of bacteria. Interestingly, the HRP immunodetection assay indicated that IcsA levels on the surface of the *ompA* mutant were approximately 53.5 ± 6.5% (ratio 0.23) compared to that of wild-type bacteria (ratio 0.43) (Fig. 26D). As expected, pOA complementation significantly restored wild-type levels (81.4 ± 7.2; ratio 0.35). The amount of IcsA on the bacterial surface was also determined by quantitative dot-blot analysis. In agreement with the results of HRP enzymatic activity, the levels of IcsA on the bacterial surface, as measured by densitometry analysis, were found to be reduced to 51.5 ± 5.9% of the wild-type strain, while pOA complementation increased these levels to 82.4 ± 4.8% (Fig. 26C). Taken together, these results clearly indicated that the *ompA* mutant displayed reduced levels of antibody-accessible IcsA on the bacterial surface, that this reduction did not negatively influence the fractions of released IcsA* and of membrane-bound ca-IcsA*, and that it was indeed due to the lack of OmpA.

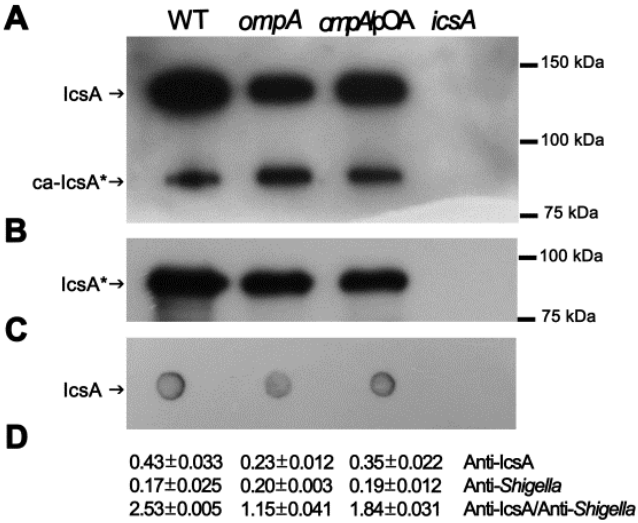

Fig. 26. The lack of OmpA influenced IcsA expression. Western blot analysis of WCE (A) and supernatants (B) of exponentially-growing wild-type strain (WT), the *ompA* mutant strain HND92 (*ompA*), the pOA-complemented derivative strain (*ompA*/pOA) and of the *icsA* mutant strain SC560 (*icsA*). Blots were probed with an anti-IcsA antiserum. The positions of the full length mature IcsA (IcsA) of IcsP-cleaved fragment (IcsA*) and of cell associated IcsA* (ca-IcsA*), are indicated by arrows at the left side. Quantitative surface immunodetection of IcsA: (C) dot blots of intact bacteria probed with anti-IcsA antibody; and (D) intact bacteria were treated with anti-IcsA and anti-*S. flexneri* antibodies. The amount of antibody bound to the bacterial surface was determined by labelling with HRP-conjugated secondary antibody and measuring the HRP enzymatic activity (OD_{370}). Means and standard deviation of three independent experiments are shown. Blots are representative. Size markers (kDa) are shown at the right side.

Membrane permeability of the *ompA* mutant

OmpA has been shown to play an important role in maintaining OM integrity of *E. coli* (Prasadarao *et al.*, 1996, Wang, 2002). To study the effect of the lack of OmpA on membrane integrity of *S. flexneri*, we used

the LIVE/DEAD BacLight kit (Invitrogen). Although this kit is commonly used to discriminate between active and dead bacteria, it is also used to differentiate between bacteria presenting intact or damaged membranes. The kit is composed of a mixture of the green- and red-fluorescent nucleic acid stains SYTO9 and propidium iodide (PI), respectively. The two fluorescent molecules differ both in their spectral characteristics and in the ability to penetrate bacterial cells. While SYTO9 enters all cells, PI enters only bacteria presenting altered membrane permeability. When used in combination, the presence of bacteria presenting defects in membrane integrity causes a reduction in the green fluorescence emission (Haugland, 1996). Therefore, exponentially-growing bacteria were stained with a mixture of the fluorescent dyes and the emitted fluorescence was measured and expressed in arbitrary fluorescence intensity units (see Materials and Methods for details). The results obtained indicated that while the wild-type strain displayed a green/red ratio of 20.3 ± 1.2 units, the *ompA* mutant scored 12.3 ± 1.0, indicating increased membrane permeability ($P < 0.01$). The defect in membrane permeability was due to the lack of OmpA since complementation with pOA, increased the green/red ratio to 19.8 ± 1.1 units, a value comparable to that of the wild-type strain. These data indicated that OmpA is required for *S. flexneri* membrane integrity.

OmpA is not required for host cytosolic phospholipase A2 activation

Several reports have highlighted the involvement of OmpA in pathogen-host-cell interactions (Krishnan and Prasadarao, 2012, Maruvada and Kim 2011). Recently, it has been reported that activation of host cytosolic phospholipase A2 (cPLA2α) is important for host cell invasion as well as for triggering cell cytoskeletal rearrangements (Kandzari *et al.*, 1996). In particular, using human brain microvascular endothelial cultured cells as a model to study neonatal meningitis, it has been shown that OmpA of an *E. coli* K1 strain isolated from a patient with neonatal meningitis triggers actin condensation through activation of cPLA2α-dependent pathways [50 Maruvada R, Kim KS (2011)]. To examine whether the OmpA of *S. flexneri* is involved in the activation of cPLA2α, HeLa cell monolayers were infected (1 h of infection) with the wild-type and the *ompA* mutant strains. Western blot analysis of cellular lysates, using anti-p-cPLA2α (which recognizes the phosphorylated active form of cPLA2α) and anti-cPLA2α (which recognizes both the active and the inactive forms of cPLA2α) polyclonal antibodies, failed to display differences between the *ompA* mutant and the wild-type strain (Fig. S2). These results seemed to

exclude that OmpA of *S. flexneri* could be involved in the activation of cPLA2α.

Discussion

Homeostasis of the intestinal epithelial barrier is subverted by crosstalks between enteric bacterial pathogens and mucosal tissues. The genetic make up of bacterial enteric pathogens can be seen in the perspective of a coevolutionary process that has led to the presence of genes encoding effectors able to overcome the innate immune response. This intricate mechanism leads to modulation of host inflammatory response launching a successful colonization.

S. flexneri synthesizes a variety of effectors that are secreted via the T3SS directly into host cells in order to modulate cellular signalling pathways and to subvert host innate immune responses. The hallmark of *S. flexneri* infection is the induction of a heavy host inflammatory response and to massive recruitment of PMNs at the site of infection that initially contributes to increase bacterial invasion of the intestinal mucosa. On the contrary, at late stages of infection *S. flexneri* reduces inflammation to prevent premature clearance from host tissues to prolong its proliferation. The principal actors in modulating inflammatory response are the *S. flexneri* Osp and IpaH effector proteins (Shames and Finlay, 2012).

In this work the role of the *ospB-phoN2* operon in the pathogenesis of *S. flexneri* has been studied. Here we show that the T3SS secreted effector OspB plays a pivotal role in the inflammatory response elicited by *S. flexneri* at the early stages of infection. By performing Serény tests (Sereny, 1957), we demonstrated that OspB is required for full induction of the inflammatory response during *S. flexneri* infection of the conjunctiva of guinea pigs (Table 2) and, by measuring *ospB* transcriptional levels in infected HeLa cells infected, we observed that the intracellular expression of *ospB* reaches a peak at 60 min post-infection and then decreased gradually over time. This intracellular expression profile mimics that observed for the *S. flexneri ospF* gene, encoding a phosphothreonine lyase (OspF), another T3SS *S. flexneri* secreted effector involve in the modulation of inflammation (Kim *et al.*, 2008).

Basing on the *ospB* intracellular expression profile, immunofluorescence experiments were performed to evaluate the intracellular localization of OspB. The results of these experiments revealed that OspB localized within host nucleus already 30 min post-infection. Nuclear targeting is an almost common trait shared by IpaH and Osp effectors (Toyotome *et al.*, 2001; Zurawski *et al.*, 2006; Zurawski *et al.*, 2008). Nuclear translocation of OspB has been already been reported (Zurawski *et al.*, 2009), however, these authors detected OspB translocation only 4 h post-infection. Possible

explanations of this discrepancy could be the choice of the *S. flexneri* strain used in these experiments (*S. flexneri* 2a strain 2457T instead of *S. flexneri* 5a strain M90T in our experiments) and that OspB was ectopically expressed (Zurawski et al., 2009).

Interestingly, no nuclear localization signals (NLS) were detected in the deduced OspB amino acid sequence (Zurawski et al., 2009), suggesting that OspB might interact with another host protein provided with an NLS signal sequence to achieve its final nuclear destination.

The MAPK pathways of mammalian cells mediate changes in cellular gene expression in response to extracellular stimuli like pro-inflammatory or stressful stimuli. Through a phosphorylation cascade, the MAPKs target transcription factors which in turn regulate genes implied in the inflammatory response (Clark *et al.*,2003). Thus, for pathogenic bacteria, modulation of the activity of the MAPK signalling pathways is a critical event in their ability to colonize host tissues (Shan *et al.*, 2007, Bhavsar et *al.*, 2007). In this context, and based on the timing of nuclear translocation, we investigated the role of OspB in the signaling pathways of MAPKs. The results obtained revealed a significant reduction in the phosphorylation of the MAPKs Erk1/2 and p38 in Caco-2 cells infected with the *ospB* mutant already at 5 and 15 min post-infection, respectively (Fig. 6). These results indicated that OspB, during its passage through the cytoplasm to the host nucleus, likely targets cytosolic MAPKs Erk1/2 and p38 leading to their phosphorilation at early stages of infection. OspB-mediated Erk1/2 phosphorilation was reported in infected HeLa cell monolayers only 90 min post-infection (Zurawski *et al.*, 2009). Taken together these results showed that M90T induces Erk1/2 and p38 phosphorilation at early stages of infection.

The activation of MAPK signaling pathways finally leads to the induction of an inflammatory response and to PMNs migration into infected tissues. *S. flexneri* induces PMNs migration through activation of cytosolic phospholipase A2 (cPLA2) (Mumy et al., 2008). Activated-cPLA2 releases arachidonic acid from membranes where it becomes an available substrate for the 12/15-lipoxygenase (12/15-LOX) pathway and eventually to the production of hepoxilin A3 (HXA3) that, in turn, induces recruitment of PMNs at the site of infection (Mumy et al., 2008). Interestingly, it was shown that activated-Erk1/2 and -p38, individually and/or in combination are able to phosphorylate cPLA2 (Clark *et al.*, 1995; Gijòn *et al.*, 1996) In this context we hypothesized that OspB might play an important role in the mechanism of pathogenicity of *S. flexneri* by activating both Erk1/2 and p38, indirectly inducing activation of cPLA2 and by triggering HXA3

release and thus promote PMNs transmigration. Experiments are underway to experimental evidences proving that OspB is involved in the activation of cPLA2 and thus in PMNs recruitment.

In the second part of this thesis, we studied the role of *phoN2* in the mechanism of pathogenicity of *S. flexneri*. We have previously reported that PhoN2 is a virulence-associated factor of *S. flexneri* since deletion of *phoN2* lead to altered IcsA exposition at the bacterial old pole, to the formation of aberrant F-actin comet tails and to a small plaque phenotype (Santapaola *et al*., 2002; Santapaola *et al*., 2006). To get further insights we analyzed the intracellular localization of PhoN2. To this end, we generated a derivative of wild-type strain M90T (strain HNDHA10) encoding a C-terminal HA-tagged PhoN2 and, by indirect immunofluorescence experiments, we showed that PhoN2-HA displayed foci that were polarly localized (Fig. 8A). This accumulation was evidenced also in bacteria within HeLa cells (Fig. 8D), indicating that the T3SS system-dependent up-regulation of *phoN2* expression (Santapaola et al., 2002) is not required for its polar localization. Since we found polarly localized PhoN2-HA also in a *E. coli* K-12 strain complemented with pHND10 (Figure 8C; Table 1), we concluded that both *S. flexneri* and *E. coli* K-12 strains share a conserved mechanism for PhoN2 transport and storage, likely through the presence of common periplasmic accessory factor(s).
The finding that PhoN2 was polarly localized, just beneath the IcsA cap in the great majority of immunostained fluorescent bacteria (Figure 9A), led us to ascertain whether IcsA participated in PhoN2-HA polar localization. Since we found PhoN2-HA polarly localized in a S. flexneri icsA mutant (strain SC560) complemented with the phoN2::HA gene, we concluded that IcsA was not required for the polar localization of PhoN2.
Next, to evaluate the mechanism by which PhoN2 localized at bacterial poles we analyzed its amino acid sequence, searching for motif driving its localization. A deletion and specific amino acid substituted derivatives of PhoN2-HA were generated and analyzed for their ability to polarly localize. We observed that, a deletion encompassing the DNA region encoding the N-terminal PPPP motif (plasmid pHND11$_{\Delta 79\text{-}223}$; Table 1) presented PhoN2-HA homogenously distributed in the immunostained bacteria and abrogated apyrase activity (Fig. 10). Conversely the introduction of an amino acid specific substitution in the catalytic site, known to abrogate enzymatic activity, led to the correct polar localization of the protein clearly indicating that the apyrase catalytic activity is not involved in the process of PhoN2 polar localization.

To further characterize the role of the PPPP motif, we introduced specific amino acid substitutions replacing each proline residue with a serine residue. The analysis of the mutated derivatives of PhoN2-HA clearly indicated that substitution of the first and of the second proline residue did not alter its periplasmic delivery, polar localization and apyrase activity (Fig. 11). Remarkably, substitutions of the third and fourth proline residues presented a lower level of protein expression and the substitution of the fourth proline residue led to aberrant cytoplasmic accumulation of PhoN2 and inhibited its enzymatic activity. These observations prompted us to analyze the stability of the mutated PhoN2 derivatives. As expected, the constructs carrying the substituted third and fourth proline residues presented an high degree of protein instability. Remarkably, the recombinant PhoN2-HA protein harboring the third P to S substitution was almost correctly delivered into the periplasmic compartment and, even at lower-extent, displayed PhoN2-HA polarly localized foci and was able to complement apyrase activity (Fig. 11). These results indicated that the PPPP motif plays a pivotal role in PhoN2 stability and thus in PhoN2 structural conformation.

Structural analysis of the acid phosphatase PhoN, from *S. typhimurium*, that like PhoN2, belongs to the class A of the NSAPs, suggested a possible specific interaction between the C-terminal PPPP motif and an invariant Y residue (Y154 in PhoN, Y155 in PhoN2) next to the D1 domain, stabilizing the structure of the catalytic site (Ishikawa *et al*., 2000, Makde *et al*., 2007). To prove this hypothesis, we analyzed the involvement of the Y155 residue of PhoN2 in its structural conformation. To this end we generated an Y155A substitution in PhoN2-HA. PhoN2 carrying the Y155A substitution failed to express apyrase activity and displayed high instability. These results showed that the PPPP motif, along with the conserved Y residue, represent fundamental elements for the architectural structure of PhoN2. Interestingly, the R192P substitution which abrogates apyrase activity had no effect on protein stability and then on the structural conformation of PhoN2.

Since PhoN2 polar localization is suggestive of possible protein-protein interactions that might assist PhoN2 in its polar delivery, we searched for specific PhoN2 interactor(s) by a two-hybrid screen in yeast. The results obtained unambiguously showed the OM protein OmpA as a strong interaction partner of PhoN2 (Table 2). We found that the binding site of OmpA corresponded to its C-terminal domain (residues 189 to 273) which is known to be exposed into the bacterial periplasm when the protein is in the eight-stranded β-barrel conformation (Koebnik and Kramer, 1995;

Smith et al., 2007). The interaction between PhoN2 and OmpA was confirmed by in vivo formaldehyde cross-linking experiments (Fig. 16).
Recent experimental evidence has shown that OmpA is a pore that may adopt alternative conformations, namely i) an eight-stranded β-barrel small pore with a large C-terminal domain which remains exposed into the periplasm, perhaps interacting with peptidoglycan; and ii) a 16-stranded β-barrel large pore, at physiological temperature, involving an additional eight β-strands from the C-terminal domain (Zakharian and Reusch, 2003, Zakharian and Reusch, 2005, Smith *et al.*, 2007, Khalid *et al.*, 2008). Therefore, our results clearly indicated that PhoN2 binds to the periplasmic exposed C-terminal domain of OmpA when this protein is in the eight-stranded β-barrel small pore conformation. Noteworthy, albeit OmpA is the interactor of PhoN2, it is not required for the polar localization of PhoN2, since we found PhoN2-HA polarly localized in a S. flexneri ompA mutant. (Figure 17). Analysis of the amino acid sequence of OmpA led us to identify a polyproline stretch (^{183}PAPAP^{187}) located in the C-terminal domain of OmpA. Trough a computational modeling of protein-protein interaction we hypothesized that this PAPAP stretch could substitute the PPPP motif of PhoN2 interacting with the invariant Y155 residue, stabilizing PhoN2-OmpA complex. Cross-linking experiments revealed the formation of a molecular complex between PhoN2 and the mutated derivative of OmpA. These results led us to conclude that the PAPAP motif is likely not involved in the PhoN2-OmpA interaction or that regions other than the PAPAP motif concurred in the interaction with PhoN2. Experiments based on the two-hybrid assay, using selected truncated OmpA polypeptides as baits, are underway to determine key residues involved in the interaction with PhoN2.
OmpA is a multifunctional major OM protein of *E. coli* and other enterobacteria (Reusch, 2012). Since OmpA interacts with the virulence factor PhoN2 and it has been recently reported that OmpA as a relevant virulence factor in the pathogenesis of various infectious diseases (Krishnan and Prasadarao, 2012), we studied the role of OmpA in the pathogenesis of *S. flexneri*. Moreover, it has been recently reported that OmpA of *S. flexneri* is recognized by the Toll-like receptor 2, indicating that OmpA could play a pivotal role in initiating host innate and adaptive immune responses, thus representing a potential vaccine candidate (Pore *et al*., 2012).
To unravel its role, an *ompA* mutant (strain HND92) of the wild-type *S. flexneri* 5a strain M90T was generated (Table 1). HND92 was able to bind Congo red, did not present growth differences with parental strain and it was able to invade cultured epithelial cells, although the percentage of

HeLa cells that were invaded by the *ompA* mutant was significantly lower than wild-type. On the contrary, the number of intra-cellular bacteria was higher than the number of wild-type. This phenotype was highly reminiscent of *S. flexneri* mutants presenting altered cell-to-cell spread (Bernardini *et al.*, 1989, Suzuki *et al.*, 1994). Moreover, the lack of OmpA did not affect IpaABCD synthesis and secretion and the formation of apparently proper F-actin comet tails (Figs 20 and 22), indicating that the lack of OmpA had no influence on the activation of the T3SS system as well as on the IcsA-mediated activation of actin-nucleating proteins.

Indeed, the *ompA* mutant was totally impaired in cell-to-cell spread since it was unable to plaque on HeLa cell monolayers (Fig. 23). The inability to plaque was likely due to the dramatically reduced levels of protrusion formation, seen in HeLa cells infected with the *ompA* mutant. Moreover, the intra-cellular distribution of the *ompA* mutant was considerably different to that of wild-type. Bacteria did not display the classical random distribution of wild-type, while appeared to be entrapped within the cytoplasm (Fig. 21, insets). Wild-type plaque size, proper intra-cellular distribution and protrusion formation were restored by complementing with plasmid pOA (Table 1), indicating that OmpA is required for of *S. flexneri* intra- and inter-cellular spread. These findings prompted us to evaluate IcsA exposition by indirect immunofluorescence. Noteworthy, the *ompA* mutant displayed IcsA exposed across the entire bacterial surface (Fig. 25), with evident IcsA polar reinforcements noticed in the majority of immunostained bacteria. We hypothesized that the presence of these IcsA polar reinforcements may account for the ability of the *ompA* mutant to form apparently normal F-actin comet tails. The aberrant exposition of IcsA on the entire bacterial surface was not due to increased IcsA expression since we unexpectedly detected even lower levels of the 110-kDa mature IcsA in WCE of the *ompA* mutant (56.6 ± 4.8%), compared to wild-type (Fig. 26A).

Intact LPS molecules (smooth LPS) are important for virulence of *S. flexneri* and O antigen polysaccharide chains have been shown to influence IcsA exposition on the bacterial surface and ABM within host cells (Morona and Van Den Bosch, 2003; Van Den Bosch and Morona, 2003). The inability of the *ompA* mutant to plaque and IcsA exposition across the entire bacterial surface are phenotypes reminiscent of rough LPS mutants, although rough mutants have been reported to be unable to form proper F-actin comet tails (Morona and Van Den Bosch, 2003; Van Den Bosch and Morona, 2003), a characteristic not shared by the *ompA* mutant (see above). To unravel this point, the LPS structure of the *ompA* mutant was evaluated

and compared to that of the parental strain either indirectly, by determining the resistance to NHS which is known to correlate with a smooth LPS, or directly by silver staining of LPS preparations. Since the *ompA* mutant presented the same level of resistance to NHS and displayed the same LPS structure of the parental strain (Figure 24), we excluded that the inability to plaque and to present IcsA exposed across the entire bacterial surface of the *ompA* mutant was due to altered LPS biosynthesis.

The current model of the distribution of IcsA on the S. flexneri OM indicates that, following its secretion through the Sec translocon, IcsA is strictly delivered and inserted into the OM at the old bacterial pole by the aid of specific proteins that recognize and bind to IcsA (Goldberg *et al.*, 1993, Charles *et al*., 2001, Robbins *et al.*, 2001, Brandon et al., 2003, Wagner et al., 2009). Subsequently, membrane-bound IcsA diffuses to lateral bacterial surface by membrane fluidity, forming a gradient that decreases in concentration with distance from the old pole and OM protease, IcsP, is thought to be involved in the sharpening of the IcsA gradient (Tanji *et al.*, 1992, Robbins *et al.*, 2001). IcsA at lateral bacterial surface is likely masked by LPS molecules, probably in combination with specific OM proteins, in order to hamper its function in ABM at those sites (Morona and Van Den Bosch, 2003, Morona *et al.*, 2003). To explain the formation of typical IcsA caps in S.flexneri it has been hypothesized that LPS molecules of shorter length may be preferentially localized at the old cell pole, thus allowing exposition and function of IcsA only at this site (Morona *et al.*, 2003).

Mutations that alter the synthesis or assembly of any of the OM components may cause permeability defects (Wu et al., 2005). OmpA, an extremely abundant protein (about 100.000 molecules/cell), has been shown to play an important role in maintaining *E. coli* OM integrity (Prasadarao *et al.*, 1996, Wang, 2002, Smith *et al.*, 2007). By using a fluorescence approach, we have shown that the lack of OmpA increased membrane permeability of *S.flexneri* (Krishnan and Prasadarao, 2012). Although the mechanisms for targeting and assembling proteins into the OM are largely unknown, it is possible to envisage that the lack of OmpA may have considerably altered the homeostatic control mechanism that coordinates the overall OM assembly process in *S. flexneri* (Smith *et al.*, 2007). In this context, it is conceivable that alteration of the OM composition due to the lack of OmpA, likely mislocalized newly synthesized lipids (LPS and phospholipids) as well as OM proteins, so that only a fraction of mature IcsA undergoes proper insertion into the OM. We hypothesized that the fraction of mature IcsA molecules which are not

assembled into the OM might undergo protein degradation, thus accounting for the reduced IcsA expression seen in the *ompA* mutant. In line with the finding that the *ompA* mutant displayed the same LPS structure of the parental strain, it is conceivable to hypothesize OmpA as a possible LPS interactor required for the masking of mature IcsA at lateral bacterial surface.

Noteworthy, while the aberrant IcsA exposition across the bacterial surface did not influence the ability of IcsA to interact with host proteins vinculin and N-WASP to nucleate F-actin polymerization only in correspondence of the old bacterial pole (where we found IcsA polar reinforcements; see above), the lack of OmpA dramatically affected protrusion formation (Fig. 21). Although ABM is absolutely required for protrusion formation in *Shigella* spp., the specific molecular mechanisms are poorly understood (Haglund and Welch, 2011). It has been recently suggested that an actin nucleation process, independent of the Arp2/3 complex, may be involved in productive protrusion formation (Heindl *et al.*, 2010). One intriguing possibility is that OmpA of *S. flexneri* might also interact, directly or indirectly, with specific host proteins to trigger invasion of neighbouring cells. Several host proteins like the Diaphanous formin Dia, ezrin, vinculin, and cadherins have been reported to be implicated in the process of protrusion-mediated cell-to-cell spread of *Shigella* spp. (Haglund and Welch, 2011). Experiments are underway to evaluate the importance of the interactions between OmpA and these host proteins in the process of protrusion formation.

Moreover, OmpA interaction with host cPLA2α has been also reported (Maruvada and Kim, 2011). Apart from its role in liberating arachidonic acid from membrane phospholipids, cPLA2α has been shown to be important for host cell invasion as well as for triggering host cell cytoskeletal rearrangements (Kandzari et al., 1996, Maruvada and Kim, 2011). In particular, it has been demonstrated that OmpA of a neonatal meningitis causing *E. coli* K1 strain triggers actin condensation via activation of cPLA2α-dependent pathways (Maruvada and Kim, 2011). On this basis, we compared the ability of the *ompA* mutant and of the wild-type strains to activate cPLA2α. Since no difference in cPLA2α activation was observed in extracts of HeLa cells infected with the two strains (Figure S2), we concluded that, differently from the *E. coli* K1 strain, the OmpA of *S. flexneri* was not involved in cPLA2α activation.

The production of apparently normal F-actin comet tails displayed by the *ompA* mutant is in contrast with previous studies reporting that *S. flexneri* mutants displaying IcsA exposed across the bacterial surface presented

aberrant bacterial motility (Morona and Van Den Bosch, 2003; Van Den Bosch and Morona, 2003). To explain this discrepancy, we argued that the apparently normal F-actin comet tails, displayed by the *ompA* mutant, might be ineffective to generate those unidirectional movements which have been shown to be necessary for productive protrusion formation. This hypothesis is supported by the findings that not-polarly exposed IcsA drastically affects the force of actin-based motility necessary to deform the plasma membrane thus leading to protrusion formation (Monack and Theriot, 2001). Therefore, we envisaged that the apparently normal F-actin comet tails, displayed by the ompA mutant, are not effective to generate productive protrusion formation, thereby blocking the mutant within the cytoplasm.

Moreover, the observed phenotype of the *ompA* mutant was reminiscent of that displayed by a *mlaA*/*vacJ S. flexneri* mutant (*mlaA*/*vacJ* encodes a lipoprotein exposed on the bacterial surface) (Suzuki *et al.*, 1994). It has been reported that the *mlaA*/*vacJ* mutation, generated into the *S. flexneri* 2a strain YSH600T, did not affect the ability of S. *flexneri* to invade and to multiply within infected MK2 cells and to form protrusions at a rate similar if not identical to that of the wild-type strain, while the *mlaA*/*vacJ* mutant was unable to plaque and presented increased membrane permeability. The authors reported that the defect in plaque formation was due to the inability of the mutant to move from protrusions into the cytoplasm of adjacent cells but they did not evaluate the exposition of IcsA on the bacterial surface [41]. This latter point would have been crucial to assess similarity between these two mutants. Anyway, since the authors reported that the *mlaA*/*vacJ* mutant displayed wild-type levels of bacterium-containing membranous protrusions, while the *ompA* mutation dramatically affected protrusion formation, this difference appeared to rule out the possibility that the lack of OmpA may exert a pleiotropic effect on the expression of the *mlaA*/*vacJ* gene.

Taken together, we concluded that OmpA is required and sufficient for the expression of relevant virulence phenotypes as formation of typical IcsA caps, plaquing ability and protrusion formation and thus for intra-and inter-cellular *S. flexneri* motility (Figs 21, 23 and 25). Since the membrane architecture of the spatial arrangement of OmpA depends on the presence and on the interaction with a variety of other molecules (Smith *et al.*, 2007) we could not exclude that OmpA might play only an indirect role in the expression of these virulence phenotypes.

This study provides experimental evidences demonstrating that OmpA is a *S. flexneri* virulence factor. These findings complement the recently

discovered passive role of OmpA in the induction of the host immune responses (Pore *et al.*, 2012) strenghthening its importance also as a promising vaccine candidate.

CONCLUSIONS

In this study, we showed that OspB plays a pivotal role in the inflammatory response elicited by S.flexneri, likely acting at the early stage of infection. Our results indicates that OspB, likely during its translocation trough the cytoplasm to the nucleus, targets cytosolic MAPKs Erk1/2 and p38 leading to their activation in early stages of infection. Based on these results we would like to propose a working model by which OspB, activating Erk1/2 and p38, induces activation of cPLA2 which in turn, triggers HXA3 release and PMNs transmigration at the site of infection (Fig. 27).

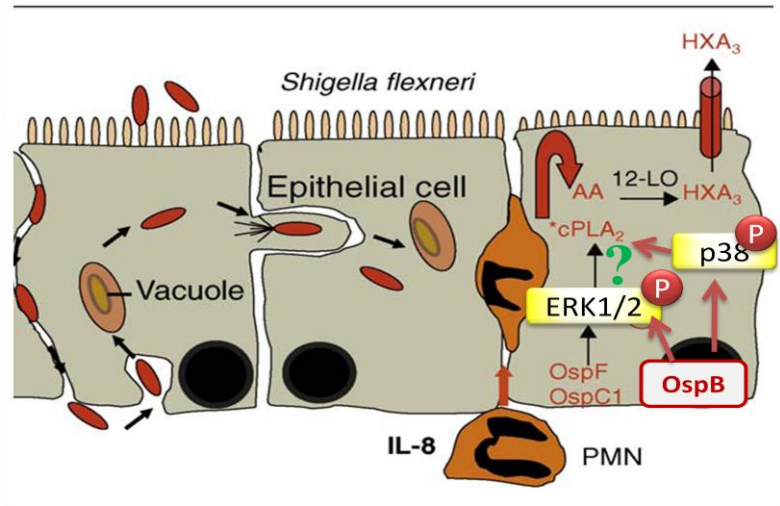

Fig. 27. Working model. Cytosolic OspB induces phosphorylation of Erk1/2 and p38, which in turn actvates cPLA2. Activated-cPLA2, by inducing the synthesis of HXA3 induces PMN migration.

Moreover, we also present experimental evidence indicating that PhoN2 and OmpA play a pivotal role in the correct insertion and exposition of IcsA in the OM. The contribution of these two protein in this process appears to be different. The lack of phoN2 led to the formation of IcsA caps considerably smaller than those of wild-type (Fig. 14). Conversely, the ompA mutant displayed IcsA exposed across the entire bacterial surface (Fig. 25).

These results led us to propose another model to try to explain the mechanism by which PhoN2 and OmpA are involved in the exposition of IcsA in the OM of S. flexneri (Fig. 28). According to this model when PhoN2 is polarly localized, its interaction with the C-terminal domain of OmpA probably stabilizes OmpA in the small pore conformation only around the old bacterial pole. This conformation allows regular exposition of IcsA at the bacterial surface and the formation of classical IcsA caps (Fig. 14). Conversely, in the absence of PhoN2, OmpA is probably present in the16-stranded β-barrel large pore structure across the bacterial length, hindering, by itself or in combination with other cell components, the exposition of IcsA. Finally, the lack of OmpA, by causing huge rearrangements of the OM, led to an mislocalization of the IcsA protein, unmasking it along the entire bacterial length (Fig. 25).

Further experiments are needed to precisely define the interaction between PhoN2 and OmpA in order to assess whether PhoN2 directly acts on the assembly process of OmpA into the OM, in its small pore conformation, or acts on the stabilization of the small pore intermediate around the old bacterial pole.

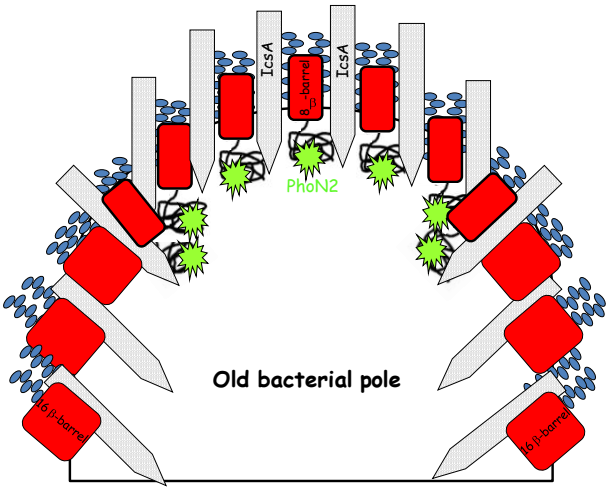

Figure 28. The interaction between PhoN2 and OmpA allows proper IcsA exposition. Representation of the model by which PhoN2 (green) may interact with OmpA (red), thus stabilizing it in its 8β-barrel conformation. This stabilization allows the formation of classical IcsA caps (dotted shape) on the OM at the old bacterial pole.

References

- Ansai T, Chen X, Barik S, Takehara, T (2002) Conserved proline residues near the N-terminus are important for enzymatic activity of class A bacterial acid phosphatases. Arch Biochem Biophys 408:144–146.
- Baba T, Ara T, Hasegawa M, Takai Y, Okumura Y, Baba M, Datsenko KA, Tomita M, Wanner BL, Mori H (2006) Construction of *Escherichia coli* K-12 in-frame, single-gene knockout mutants: the Keio collection. Mol. Syst. Biol. 2:2006.0008.
- Babu MM, Kalamalakkannan S, Subrahmanyam YVBK, Sankaran K (2002) *Shigella* apyrase-a novel variant of bacterial acid phosphatases? FEBS Lett 512:8-12.
- Berlutti F, Casalino M, Zagaglia C, Fradiani PA, Visca P, Nicoletti M (1998) Expression of the virulenceplasmid-carried apyrase gene (*apy*) of enteroinvasive *Escherichia coli* and *Shigella flexneri* is under the control of H-NS and the VirF and VirB regulatory cascade. Infect Immun 66:4957-4964.
- Bernardini ML, Mounier J, d'Hauteville H, Coquis-Rondon M, Sansonetti PJ (1989) Identification of *icsA*, a plasmid locus of *Shigella flexneri* that governs bacterial intra- and intercellular spread through interaction with F-actin. Proc Natl Acad Sci USA 86:3867–3871.
- Bhargava T, Datta S, Ramakrishnan V, Roy RK, Sankaran K, Subrahmanyam YVBK (1995) Virulent *Shigella* codes for a soluble apyrase: identification, characterization and cloning of the gene. Curr Sci 68:293-300.
- Bhavsar AP, Guttman JA, Finlay BB (2007) Manipulation of host-cell pathways by bacterial pathogens. Nature 449: 827-834.
- Buchrieser C, Glaser P, Rusniok C, Nedjari H, d'Hauteville H, Kunst F, Sansonetti PJ, Parsot C (2000) The virulence plasmid pWR100 and the repertoire of proteins secreted by the type III secretion apparatus of *Shigella flexneri*. Mol Microbiol 38:760-771.
- Charles M, Pérez M, Kobil JH, Goldberg MB (2001) Polar targeting of *Shigella* virulence factor IcsA in *Enterobacteriacae* and *Vibrio*. Proc Natl Acad Sci USA. 98:9871–9876.
- Chen X, Ansai T, Awano S, Iida T, Barik S, Takehara, T (1999) Isolation, cloning, and expression of an acid phosphatase

containing phosphotyrosyl phosphatase activity from Prevotella intermedia. J Bacteriol 181:7107–7114.

- Clark AR, Dean JL, Saklatvala J (2003) Post-transcriptional regulation of gene expression by mitogen-activated protein kinase p38. FEBS Lett. 546:37-44.
- Clark JD, Schievella AR, Nalefski EA, Lin LL (1995) Cytosolic phospholipase A2. J Lipid Mediat Cell Signal. 12:83-117.
- Clerc P, Sansonetti PJ (1987) Entry of *Shigella flexneri* into HeLa cells: evidence for directed phagocytosis involving actin polymerization and myosin accumulation. Infect Immun 55:2681–2688.
- Cock H, van Blokland S, Tommassen J (1996) In vitro insertion and assembly of outer membrane protein PhoE of *Escherichia coli* K-12 into the outer membrane. Role of Triton X-100. J Biol Chem 271:12885–12890.
- Cossart P (2000) Actin-based motility of pathogens: the Arp2/3 complex is a central player. Cell Microbiol 2:195–205.
- Cossart P (2005) Bacterial invasion: a new strategy to dominate cytoskeleton plasticity. Dev Cell 6:314-315.
- d'Hauteville H, and Sansonetti PJ (1992) Phosphorylation of IcsA by cAMP-dependent protein kinase and its effect on intracellular spread of *Shigella flexneri*. Mol Microbiol 6:833–841.
- Datsenko KA, and Wanner BL (2000) One-step inactivation of chromosomal genes in *Escherichia coli* K-12 using PCR products. Proc Natl Acad Sci USA 97:6640–6645.
- Donnarumma G, Paoletti I, Buommino E, Fusco A, Baudouin C, Msika P, Tufano MA, Baroni A (2011ù) AV119, a natural sugar from *avocado gratissima*, modulates the LPS-induced proinflammatory response in human keratinocytes. Inflammation. 34:568-575.
- Fixen KR, Janakiraman A, Garrity S, Slade DJ, Gray AN, Karahan N, Hochschild A, Goldberg MB. (2012) Genetic reporter system for positioning of proteins at the bacterial pole. MBio 28:3(2). doi:pii: e00251-11. 10.1128.
- Egile C, d'Hauteville H, Parsot C, Sansonetti PJ (1997) SopA, the outer membrane protease responsible for polar localization of IcsA in *Shigella flexneri*. Mol Microbiol 23:1063-1073.
- Fukuda I, Suzuki T, Munakata H, Hayashi N, Katayama E, Yoshikawa M, Sasakawa C (1995) Cleavage of *Shigella* surface

protein VirG occurs at a specific site, but the secretion is not essential for intracellular spreading. J Bacteriol 177:1719–1726.

- Gijòn M, Qiu Z, Leslie C. (1996) Activation of JUN kinases and p38 in macrophages and phosphorylation of cytosolic phospholipase A2. FASEB J. 10, A978.
- Goldberg MB (2001) Actin-based motility of intracellular microbial pathogens. Microbiol Mol Biol Rev 65: 595–626.
- Goldberg MB, Bârzu O, Parsot C, Sansonetti PJ (1993) Unipolar localization and ATPase activity of IcsA, a *Shigella flexneri* protein involved in intracellular movement. J Bacteriol 175:2189–2196.
- Goldberg MB, Theriot JA, Sansonetti PJ (1994) Regulation of surface presentation of IcsA, a *Shigella* protein essential to intracellular movement and spread, is growth phase dependent. Infect Immun 62:5664–5668.
- Guzman LM, Belin D, Carson MJ, Beckwith J (1995) Tight regulation, modulation, and high-level expression by vectors containing the arabinose P_{BAD} promoter. J Bacteriol 177:4121-4130.
- Haglund CM, Welch MD (2011) Pathogens and polymers: microbe-host interactions illuminate the cytoskeleton. J Cell Biol 195:7–17.
- Hale TL, Formal SB (1981) Protein synthesis in HeLa or Henle 407 cells infected with *Shigella dysenteriae* 1, *Shigella flexneri* 2a, or *Salmonella typhimurium* W118. Infect Immun 32:137–144.
- Haugland RP (1996) Handbook of fluorescent probes and research chemicals. 6th ed, Eugene, Oreg, Molecular Probes Inc.
- Hazan-Halevy I, Seger R, Levy R (2000) The requirement of both extracellular regulated kinase and p38 mitogen-activated protein kinase for stimulation of cytosolic phospholipase A2 activity by either FcgRIIA or FcgammaRIIIB in human neutrophils. A possible role for Pyk2 but not for the Grb2-Sos-Shc complex. J Biol Chem 275:12416-23.
- Heindl JE, Saran I, Yi CR, Lesser CF, Goldberg MB (2010) Requirement for formin-induced actin polymerization during spread of *Shigella flexneri*. Infect Immun 78:193–203.
- Hitchcock PJ, Brown TM (1983) Morphological eterogeneity among *Salmonella* lipopolysaccharide chemotypes in silver-stained polyacrylamide gels. J Bacteriol 154:269–277.

- Hofstra H, Van Tol MJD, Dankert J (1980) Crossreactivity of major outer membrane proteins in *Enterobacteriaceae* studied by crossed immunoelectrophoresis. J Bacteriol 143:328-337.
- Hong M, Payne SM (1997) Effect of mutations in *Shigella flexneri* chromosomal and plasmid-encoded lipopolysaccharide genes on invasion and serum resistance. Mol Microbiol 24:779-791.
- Huber J, Fürnkranz A, Bochkov VN, Patricia MK, Lee H, Hedrick CC, Berliner JA, Binder BR, Leitinger N (2006) Specific monocyte adhesion to endothelial cells induced by oxidized phospholipids involves activation of cPLA2 and lipoxygenase. J Lipid Res. 47:1054-1062.
- Ishikawa K, Mihara Y, Gondoh K, Suzuki E, Asano Y (2000) X-ray structures of a novel acid phosphatase from *Escherichia blattae* and its complex with the transition-state analog molybdate. EMBO J 19:2412–2423.
- Kadurugamuwa JL, Rohde M, Wehland J, Timmis KN (1991) Intercellular spread of *Shigella flexneri* through a monolayer mediated by membranous protrusions and associated with reorganization of the cytoskeletal protein vinculin. Infect Immun 59:3463–3471.
- Khalid S, Bond PJ, Carpenter T, Sansom MS (2008) OmpA: gating and dynamics via molecular dynamics simulations. Biochim Biophys Acta 1778:1871–80.
- Kim DW, Chu H, Joo DH, Jang MS, Choi JH, Park SM, Choi YJ, Han SH, Yun CH (2008). OspF directly attenuates the activity of extracellular signal-regulated kinase during invasion by *Shigella flexneri* in human dendritic cells. Mol. Immunol. 45:3295-3301.
- Koebnik R, Kramer L (1995) Membrane assembly of circularly permuted variants of the *E. coli* outer membrane protein OmpA. J Mol Biol 250:617–626.
- Kohler H, Rodrigues SP, McCormick BA (2002) *Shigella flexneri* interactions with the basolateral membrane domain of polarized model intestinal epithelium: role of lipopolysaccharide in cell invasion and in activation of the mitogen-activated protein kinase ERK. Infect Immun 70:1150–1158.
- Krishnan S, Prasadarao NV (2012) Outer membrane protein A and OprF: versatile roles in Gram-negative bacterial infections. FEBS J. doi: 10.1111/j.1742-4658.2012.08482.x.

- Labrec EH, Schneider H, Magnani TJ, Formal SB (1964) Epithelial cell penetration as an essential step in the pathogenesis of bacillary dysentery. J Bacteriol 88:1503–1518.
- Laemmli UK (1970) Cleavage of structural proteins during the assembly of the head of bacteriophage T4. Nature 227:680–685.
- Le Gall T, Mavris M, Martino MC, Bernardini ML, Denamur E, Parsot C (2005) Analysis of virulence plasmid gene expression defines three classes of effectors in the type III secretion system of *Shigella flexneri*. Microbiology151:951–962.
- Lin LL, Wartmann MA, Lin Y, Knopf JL, Seth A, Davis RJ (1993) cPLA2 is phosphorylated and activated by MAP kinase. Cell. 72:269-278
- Livak KJ, Schmittgen TD (2001) Analysis of relative gene expression data using real-time quantitative PCR and the 2(−Delta Delta C(T)) Method. Methods 25:402–408.
- Makde RD, Mahajan SK, Kumar V (2007) Structure and mutational analysis of the PhoN protein of *Salmonella typhimurium* provide insight into mechanistic details. Biochemistry 46:2079–2090
- Makino S, Sasakawa C, Kamata K, Kurata T, Yoshikawa M (1986) A genetic determinant required for continuous reinfection of adjacent cells on large plasmid in *S. flexneri* 2a. Cell 46:551–555.
- Maruvada R, Kim KS (2011) Extracellular loops of the *Escherichia coli* outer membrane protein A contribute to the pathogenesis of meningitis. J Infect Dis 203:131-140.
- May KL, Morona R (2008) Mutagenesis of the *Shigella flexneri* autotransporter IcsA reveals novel functional regions involved in IcsA biogenesis and recruitment of host neural Wiscott-Aldrich syndrome protein. J Bacteriol 190:4666–4676.
- Miller JH (1972) Experiments in molecular genetics, p. 252–255. Cold Spring Harbor Laboratory, Cold Spring Harbor, N.Y.
- Monack DM, Theriot JA (2001) Actin-based motility is sufficient for bacterial membrane protrusion formation and host cell uptake. Cell Microbiol 3:633-647.
- Morona R, Daniels C, Van Den Bosh L (2003) Genetic modulation of *Shigella flexneri* 2a lipopolysaccharide O antigen modal chain length reveals that it has been optimized for virulence. Microbiology 149:925–939.

- Morona R, Van Den Bosch L (2003) Lipopolysaccharide O antigen chains mask IcsA (VirG) in *Shigella flexneri*. FEMS Microbiol Lett 221:173–180.
- Mumy KL, Bien JD, Pazos MA, Gronert K, Hurley BP, McCormick BA (2008) Distinct isoforms of phospholipase A2 mediate the ability of *Salmonella enterica* serotype typhimurium and *Shigella flexneri* to induce the transepithelial migration of neutrophils. Infect Immun 76:3614–3627.
- Neibuhr K, Ebel F, Frank R, Reinhard M, Domann E, Carl UD, Walter U, Gertier FB, Weheland J, Chakraborty T 1997. A novel proline-rich motif present in ActA of *Listeria monocytogenes* and cytoskeletal proteins is the ligand for the EVH1 domain, a protein module present in the Ena/VASp family. EMBO J 16:5433-5444.
- Nicoletti M, Santino I, Petrucca A, Del Chierico F, Cannavacciuolo S, Casalino M, Sessa R, Cipriani P (2008) Evaluation by real-time PCR of the expression of *S. flexneri* virulence-associated genes *ospB* and *phoN2* under different genetical backgrounds. Int J Immunopathol Pharmacol 21:707-714.
- Oaks EV, Wingfield ME, Formal SB (1985) Plaque formation by virulent *Shigella flexneri*. Infect Immun 48:124–129.
- Pore D, Chowdhury P, Mahata N, Pal A, Yamasaki S, Mahalanabis D, Chakrabarti MK (2009) Purification and characterization of an immunogenic outer membrane protein of *Shigella flexneri* 2a. Vaccine 27:5855–5864.
- Pore D, Mahata N, Chakrabarti MK (2012) Outer membrane protein A (OmpA) of *Shigella flexneri* 2a links innate and adaptive immunity in a TLR2-dependent manner and involvement of IL-12 and nitric oxide. J Biol Chem 287:12589–12601.
- Prasadarao NV, Wass CA, Weiser JN, Stins MF, Huang SH, Kim KS (1996) Outer membrane protein A of *Escherichia coli* contributes to invasion of brain microvascular endothelial cells. Infect Immun 64:146-153.
- Purdy GE, Fisher CR, Payne SM (2007) IcsA surface presentation in *Shigella flexneri* requires the periplasmic chaperones DegP, Skp, and SurA. J Bacteriol 189:5566–5573.
- Rasband WS (1997–2007) ImageJ. US National Institutes of Health, Bethesda, Maryland. http://rsb.info.nih.gov/ij/.
- Rathman M, Jouirhi N, Allaoui A, Sansonetti P, Parsot C, Tran Van Nhieu G (2000) The development of a FACS-based strategy

for the isolation of *Shigella flexneri* mutants that are deficient in intercellular spread. Mol Microbiol 35:974-990.

- Reusch RN (2012) Insights into the structure and assembly of *Escherichia coli* outer membrane protein A. FEBS J. doi: 10.1111/j.1742-4658.2012.08484.x.
- Robbins JR, Monack D, McCallum SJ, Vegas A, Pham E, Goldberg MB, Theriot JA (2001) The making of a gradient: IcsA (VirG) polarity in *Shigella flexneri*. Mol Microbiol 41:861–872.
- Rossolini GM, Schippa S, Riccio ML, Berlutti F, Macaskie LE, Thaller MC (1998) Bacterial nonspecific acid phosphohydrolases: physiology, evolution and use as tools in microbial biotechnology. Cell Mol Life Sci 54:833–850.
- Sambrook J, Russel DW (2001) Molecular cloning: a laboratory manual, 3rd ed. Cold Spring Harbor Laboratory Press, Cold spring Harbor, NY.
- Sansonetti P, Egile C, Wenneras C (2001) Shigellosis: from disease symptoms to molecular and cellular pathogenesis, p.335–385. In E. A. Groisman (ed.), Principles of Bacterial Pathogenesis. Academic Press, Inc.
- Sansonetti PJ, Kopecko DJ, Formal SB (1981) Shigella sonnei plasmids: evidence that a large plasmid is necessary for virulence. Infect Immun 34:75-83.
- Sansonetti PJ, Ryter A, Clerc P, Maurelli AT, Mounier J (1986) Multiplication of *Shigella flexneri* within HeLa cells: lysis of the phagocytic vacuole and plasmid-mediated contact hemolysis. Infect Immun 51:461–469.
- Sansonetti PJ, Ryter A, Clerc P, Maurelli AT, Mounier J (1986) Multiplication of *Shigella flexneri* within HeLa cells: lysis of the phagocytic vacuole and plasmid-mediated contact hemolysis. Infect Immun 51:461–469.
- Santapaola D, Casalino M, Petrucca A, Presutti C, Zagaglia C, Berlutti F, Colonna B, Nicoletti M (2002) Enteroinvasive *Escherichia coli* virulence plasmid-carried apyrase (*apy*) and *ospB* genes are organized as a bicistronic operon and are subjected to differential expression. Microbiology 148:2519-2529.
- Santapaola D, Del Chierico F, Petrucca A, Uzzau S, Casalino M, Colonna B, Sessa R, Berlutti F, Nicoletti M (2006) Apyrase, the product of the virulence plasmid-encoded phoN2 (*apy*) gene of *Shigella flexneri*, is necessary for proper unipolar IcsA localization and for efficient intercellular spread. J Bacteriol 188:1620-1627.

- Sarli S, Nicoletti M, Schippa S, Del Chierico F, Santapaola D, Valenti P, Berlutti F (2006) Ala160 and His116 residues are involved in activity and specificity of apyrase, an ATP-hydrolyzing enzyme produced by enteroinvasive *Escherichia coli*. Microbiology 151:2853-2860.
- Sasakawa C (2010) A new paradigm of bacteria-gut interplay brought through the study of *Shigella*. Proc Jpn Acad Ser B Phys Biol Sci 86:229-243.
- Schroeder GN, Hilbi H (2008) Molecular pathogenesis of *Shigella* spp.: controlling host cell signaling, invasion, and death by type III secretion. Clin Microbiol Rev 21:134-156.
- Schweizer M, Hindennach I, Garten W, Henning U (1978) Major proteins of the *Escherichia coli* outer cell envelope membrane. Interaction of protein II with lipopolysaccharide. Eur J Biochem 82:211–217.
- Serény B (1957) Experimental keratoconjunctivitis shigellosa. Acta Microbiol Acad Sci Hung 4:367–376.
- Shan L, He P, Sheen J (2007) Intercepting host MAPK signaling cascades by bacterial type III effectors. Cell Host Microbe 1:167-174.
- Shames SR, Finlay BB (2012) Bacterial effector interplay: a new way to view effector function. Trends Microbiol. 20:214-9.
- Smith SG, Mahon V, Lambert MA, Fagan RP (2007) A molecular Swiss army knife: OmpA structure, function and expression. FEMS Microbiol Lett 273:1–11.
- Steinhauer J, Agha R, Pham T, Varga AW, Goldberg MB (1999) The unipolar *Shigella* surface protein IcsA is targeted directly to the bacterial old pole: IcsP cleavage of IcsA occurs over the entire bacterial surface. Mol Microbiol 32:367–377.
- Sugawara E, Steiert M, Rouhani S, Nikaido H (1996) Secondary structure of the outer membrane proteins OmpA of *Escherichia coli* and OprF of *Pseudomonas aeruginosa.* J Bacteriol 178:6067–6069.
- Suzuki T, Miki H, Takenawa T, Sasakawa C (1998) Neural Wiskott-Aldrich syndrome protein is implicated in the actin-based motility of *Shigella flexneri*. EMBO J 17:2767–2776.
- Suzuki T, Murai T, Fukuda I, Tobe T, Yoshikawa M, Sasakawa C (1994) Identification and characterization of a chromosomal

virulence gene, *vacJ*, required for intercellular spreading of *Shigella flexneri*. Mol Microbiol 11:31-41.

- Suzuki T, Sasakawa C (2001) Molecular basis of the intracellular spreading of *Shigella*. Infect Immun 69:5959-5966.
- Tanji K, Ohta Y, Kawato S, Mizushima T, Natori S, Sekimizu K (1992) Decrease by psychotropic drugs and local anaesthetics of membrane fluidity measured by fluorescence anisotropy in *E scherichia coli*. J Pharm Pharmacol 44:1036–1037.
- Tran CN, Giangrossi M, Prosseda G, Brandi A, Di Martino ML, Colonna B, Falconi M (2011) A multifactor regulatory circuit involving H-NS, VirF and an antisense RNA modulates transcription of the virulence gene icsA of *Shigella flexneri*. Nucleic Acids Res 39:8122-8134.
- Tsai CM, Frasch CE (1982) A sensitive silver stain for detecting lipopolysaccharides in polyacrylamide gels. Anal Biochem 119:115–119.
- Uzzau S, Figueroa-Bossi N, Rubino S, Bossi L (2001) Epitope tagging of chromosomal genes in *Salmonella*. Proc Natl Acad Sci U S A 98:15264-15269.
- Van Den Bosch L, Morona R (2003) The actin-based motility defect of a *Shigella flexneri rmlD* rough LPS mutant is not due to loss of IcsA polarity. Microb Pathog 35:11-18.
- Wagner JK, Heindl JE, Gray AN, Jain S, Goldberg MB (2009) Contribution of the periplasmic chaperone Skp to efficient presentation of the autotransporter IcsA on the surface of *Shigella flexneri*. J Bacteriol 191:815–821.
- Wang Y (2002) The function of OmpA in *Escherichia coli*. Biochem Biophys Res Commun 292:396-401.
- Waterman WH, Molski TF, Huang CK, Adams JL, Sha'afi RI (1996) Tumour necrosis factor-alpha-induced phosphorylation and activation of cytosolic phospholipase A2 are abrogated by an inhibitor of the p38 mitogen-activated protein kinase cascade in human neutrophils. Biochem. J. 319:17-20.
- Wu T, Malinverni J, Ruiz N, Kim S, Silhavy TJ, Kahne D (2005) Identification of a multicomponent complex required for outer membrane biogenesis in *Escherichia coli*. Cell 121:235-245.
- Zakharian E, Reusch RN (2003) Outer membrane protein A of *Escherichia coli* forms temperature-sensitive channels in planar lipid bilayers. FEBS Lett 555:229–235.

- Zakharian E, Reusch RN (2005) Kinetics of folding of *Escherichia coli* OmpA from narrow to large pore conformation in a planar bilayer. Biochemistry 44:6701–6707.
- Zurawski DV, Mitsuhata C, Mumy KL, McCormick BA,, Maurelli AT (2006). OspF and OspC1 are *Shigella flexneri* type III secretion system effectors that are required for postinvasion aspects of virulence. Infect Immun. 74:5964-5976.
- Zurawski DV, Mumy KL, Badea L, Prentice JA, Hartland EL, McCormick BA, Maurelli AT. (2008) The NleE/OspZ family of effector proteins is required for polymorphonuclear transepithelial migration, a characteristic shared by enteropathogenic *Escherichia coli* and *Shigella flexneri* infections. Infect Immun. 76:369-379.
- Zurawski DV, Mumy KL, Faherty CS, McCormick BA, Maurelli AT (2009) *Shigella flexneri* type III secretion system effectors OspB and OspF target the nucleus to downregulate the host inflammatory response via interactions with retinoblastoma protein. Mol Microbiol 71:350-368.